

NAG1-1201

IN-35CR

109251

P.42

Testing Of The Anemometer Circuit: Data Report

Michael J. Moen

March 15, 1992

(NASA-CR-190623) TESTING OF THE
ANEMOMETER CIRCUIT: DATA REPORT
Semiannual Status Report, period
ending 31 Dec. 1991 (Purdue Univ.)
42 p

N92-34106

Unclassified

G3/35 0109251

something different when we plot the actual frequency of the response versus the overheat. What results in Figure 32 is a fairly linear curve for each sensor. Figure 33 shows a linear curve fit for each point set. It should be kept in mind that the data only looks linear within the range of tested overheats. The important result is that if the relationship between the overheat and response frequency is truly linear, then we have not yet seen an upper limit for the frequency response of the sensor with the existing architecture. This might suggest that the best way to get a high frequency response is to turn up the overheat even higher, but then we risk burning out the sensor. An upper materials limit of the sensor was stated as an overheat of 2.5. This overheat saw a significant degradation of the film sensor. It is also important to note that not only does the smallest sensor have the highest frequency response, it also has a greater increase of frequency response with increasing overheat. Towards the end of the research, higher overheats will be tested when it is no longer such a crucial issue to burn out the sensor.

Though voltage step testing is just about finished, more analysis will be made to determine how response amplitude increases with increasing overheat and sensor size, and also as to how response frequency changes with identical overheats for different sensor sizes.

Velocity Step Test Results

Finally, in Figures 34-37 we show some results for velocity steps in the shock tube. If the curves are overlaid, it can be seen that the response shape is similar, which is encouraging for initial results. In addition, the peak amplitude does increase with increasing velocity step. As testing with the velocity step (shock tube) continues, similar analysis to what is being done with the voltage step testing will be made in order to confirm assumptions made based on voltage step testing alone. More tests are underway for the effects of changing the overheat and sensor sizes in the velocity step test.

Introduction

The following text discusses results from the electronic step testing and the beginning of velocity step testing in the shock tube. It should be kept in mind that frequency response is always measured as the time from the beginning of the event to the minimum (positive inflection) of the "bucket" that immediately follows the response. This report is not a complete account of the results from square wave testing. Some data is still in the process of being analyzed and efforts are being made to fit the data to both Freymuth's third order theory and modelled responses from SPICE circuit simulation software.

Voltage Step Test Results

Voltage step testing is initially performed using two anemometers. These anemometers are referred to simply as Anemometer I (AI) and Anemometer II (AII). Figure 1 shows a schematic of the architecture of AI. This architecture is chosen for historical reasons and has been shown to work well in various applications. Figure 2 shows a schematic of the architecture of AII. The AII architecture incorporates changes that were suggested by LaRC. These changes are (1) input isolation resistors on the op amp, (2) variable inductor on the ground side of the control resistor, (3) trim capacitor to vary the op amp rolloff and (4) resistor in series with the base of the transistor. Figure 3 shows what happens when the square wave test is applied to AI and AII using identical overheat and sensor sizes. AII exhibits a faster response than AI by about 2 μ sec, but this is before the inductor has been tuned for optimal response. Although a plot is not included, it can be shown that the variable inductor improves the response time by 2-3 μ sec for the smallest sensor on the highest tested overheat (1.7). In general the noise level is higher for AII than for AI. This might be due to stray capacitance introduced through the use of sockets for the IC's and more components than AI. However, the most desirable feature of AII is the stability of the circuit. AI has a tendency to become unstable at high overheat due to switching between negative and positive feedback. This renders it useless for testing.

Initially, AI and AII were tested at low overheat and a series of square wave tests were applied with varying amplitudes for all three sensors. Figure 4 shows an example of one sensor tested at one overheat while varying the input voltage where input voltage is measured from the function generator rather than on the board. It was determined that

if the responses were normalized by dividing the response data of any one configuration (same anemometer, sensor, overheat with varying voltage) by the peak mV response value then the curves would collapse neatly on top of each other (see Figure 5). Plotting these normalization factors against the input square wave amplitude produces a very linear curve (see Figure 6). For example, AII normalization factors for the 0.005 x 0.0005 inch sensor at an overheat of 1.19 were linearly regressed and produced an R squared value of 0.999729. The closer R squared is to 1.0, the closer the actual data is to being linear. After this result of linear normalization factors was seen identically for several configurations (no configurations deviated) it was determined that responses of any configuration could be compared regardless of the square wave amplitude as long as the data is normalized. This becomes a handy result in later analysis. As an example, Figure 7 shows the square wave response for the three different sensor sizes all tested at one square wave voltage and overheat. The actual amplitude of the response to an identical square wave increases with increasing sensor size. To get a better picture of the comparative response time, the curves are normalized (see Figure 8) with no loss in the data for response time. Figures 9-13 show the same cycle for AII at the overheat of 1.19 with the 0.005 x 0.0005 inch sensor. The input voltage is increased, the curves are normalized, then all three sensor sizes are compare at one overheat in both the normalized and non-normalized formats. As an aside, Figure 14 shows what happens to the anemometer response as the operating point reaches the current limit for the anemometer. Care must be taken to provide enough leeway for current fluctuations when setting the current limiting resistor in the anemometer. Figures 15-19 show the same cycle as before, but this time for AI at an overheat of 1.34 with the 0.005 x 0.0005 inch sensor. Figures 20-24 show the same cycle for AII at an overheat of 1.34 with the 0.005 x 0.0005 inch sensor. Figures 25-27 show the normalized responses for different sensor sizes at a single overheat. In each case, the smallest sensor has the fastest response and it begins to appear that there may be some scaling factor which relates the frequency response between the three sensor sizes. Looking at Figures 28-30, the response for a single sensor size is shown at five different overheats. At first glance, it appears that the response increases with increasing overheat, but each higher overheat sees a progressively less significant increase in the response. As we look at the data with a little more detail, results indicate that this may not be the case.

Table 1 catalogs the response time of each of the three sensors at five overheats. This data is plotted in Figure 31 for AII. Once again, the data seems to indicate that we are approaching some limiting value for the frequency response. However, we see

Anemometer I Schematic

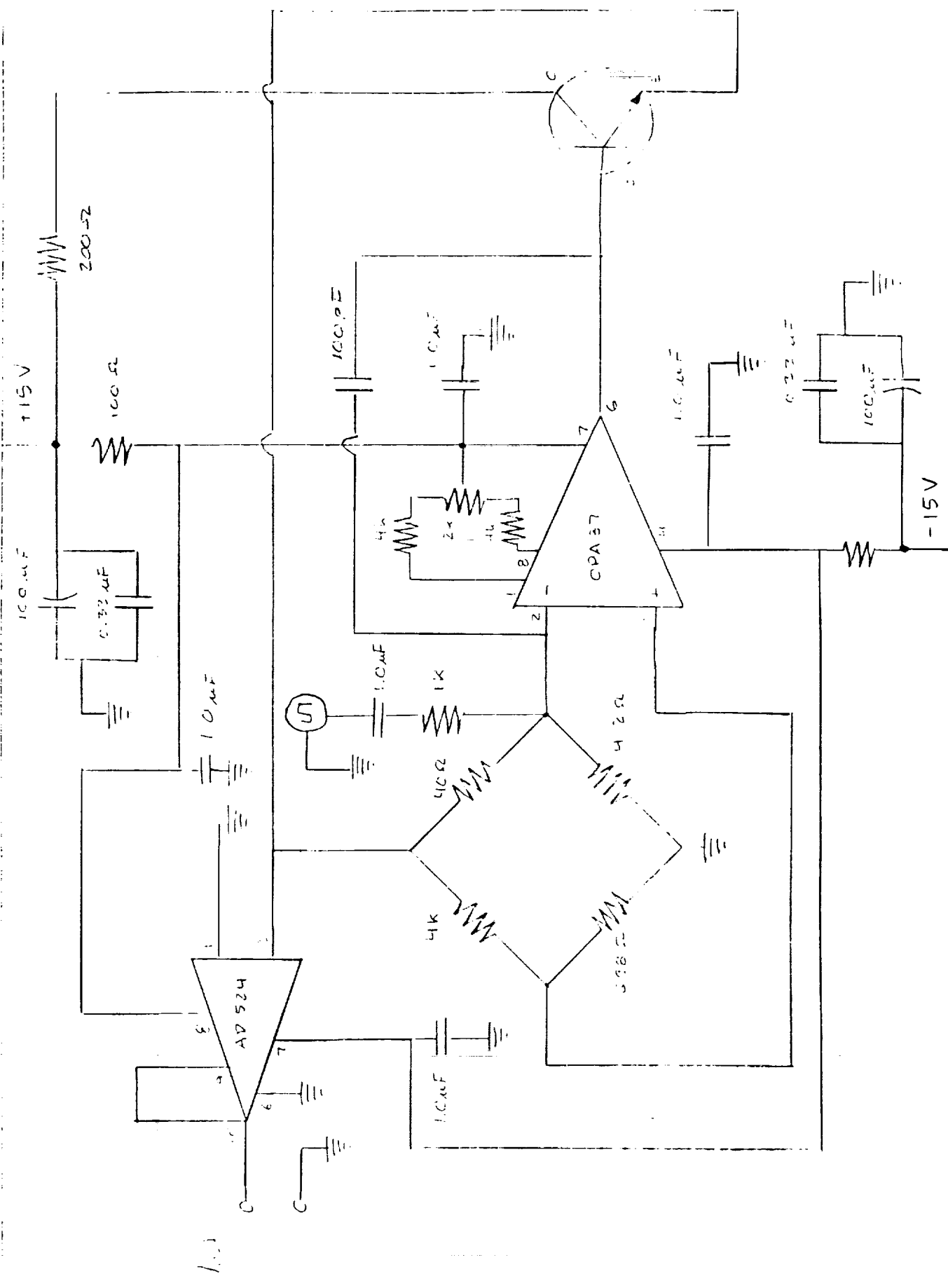
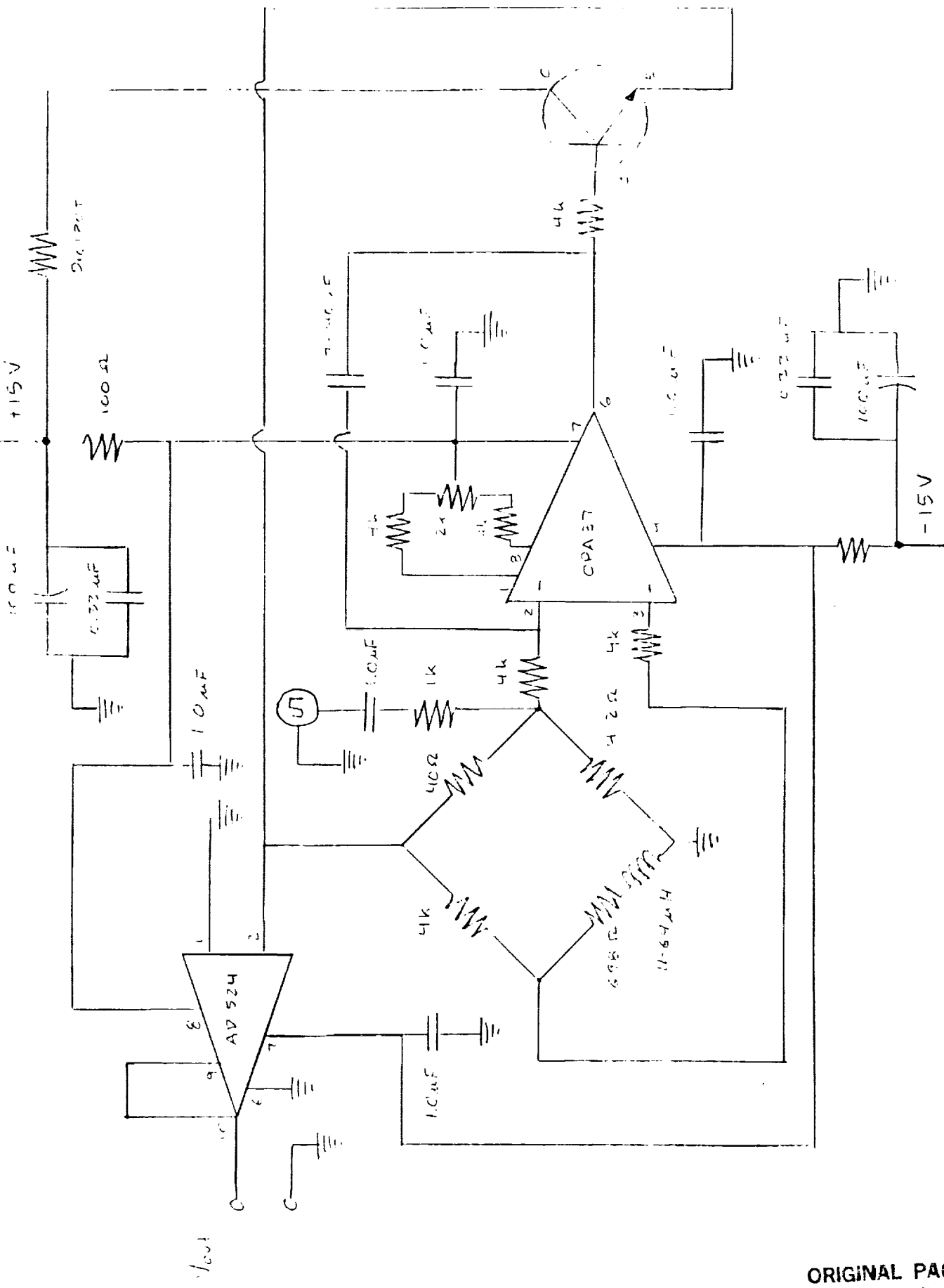


Fig 1

ORIGINAL PAGE IS
OF POOR QUALITY

Allgemeine Δ -Schematik



ORIGINAL PAGE IS
OF POOR QUALITY

**Comparison Of Response To 6 Volt Square Wave For Anemometer
Configurations I And II At Overheat 1.19**

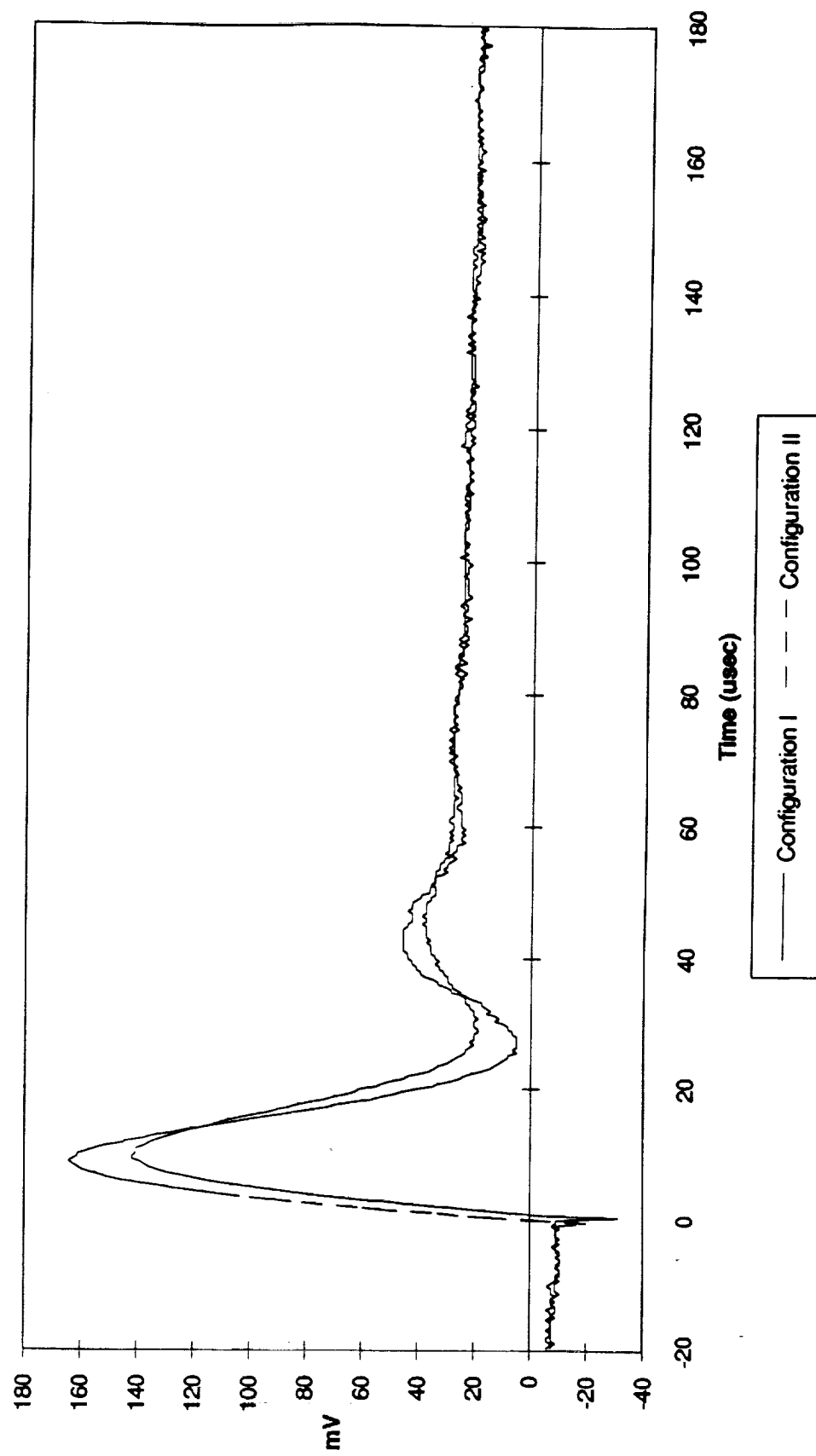


Fig. 3

Anemometer I Response To Varied Voltage Square Waves Using 0.0005 x
0.0005 Sensor At Overheat 1.19

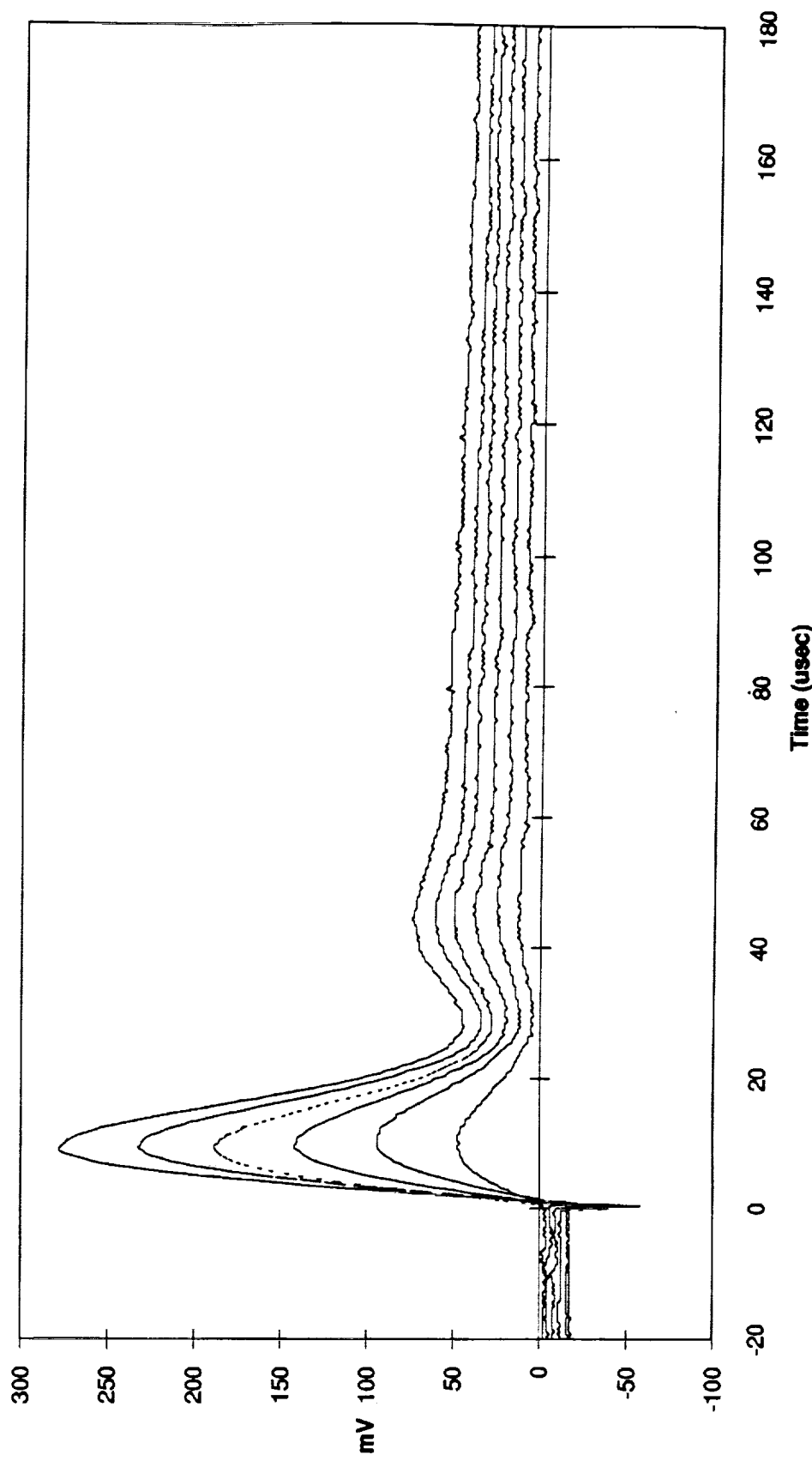


Fig 4

Anemometer I Response To Varied Voltage Square Waves Using 0.005 x
0.0005 Sensor At Overheat 1.19 (Normalized)

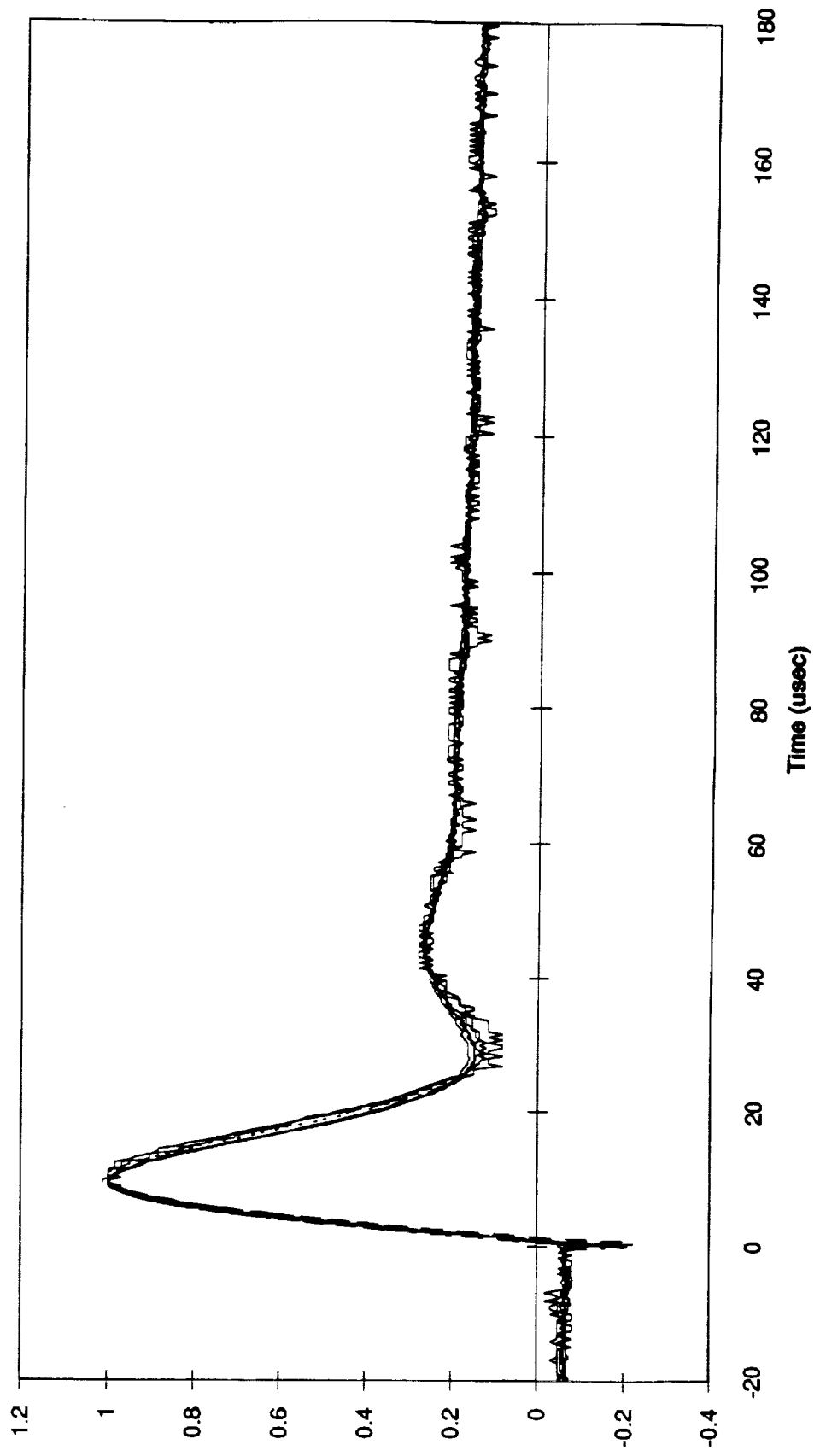


Fig 5

**Square Wave Response Normalization Factor Anemometer I Using 0.005 x
0.0005 Sensor At Overheat 1.19**

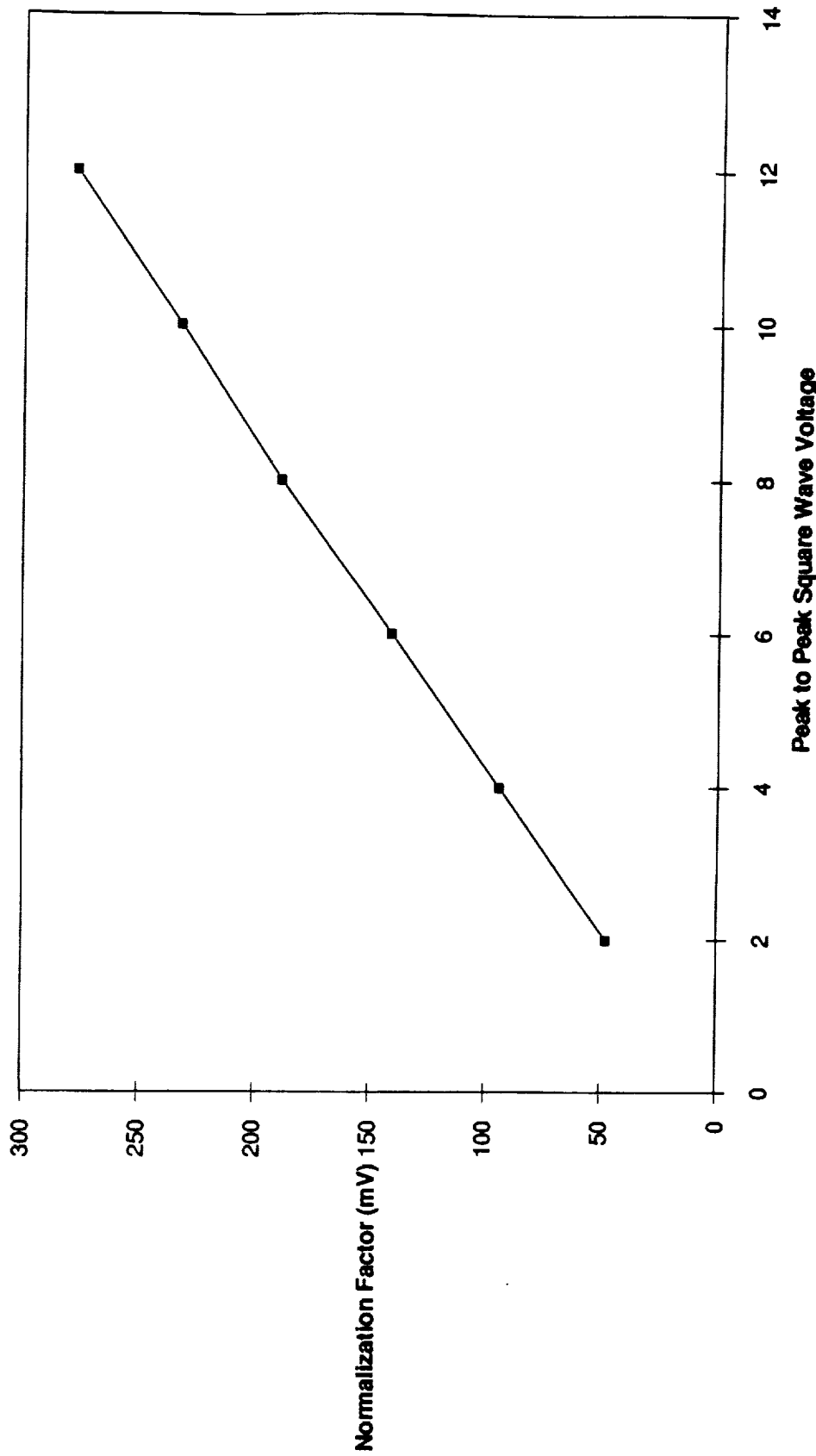


Fig 6

**Anemometer I Response To 4 Volt Square Wave For Different Sensor Sizes
(First Overheat)**

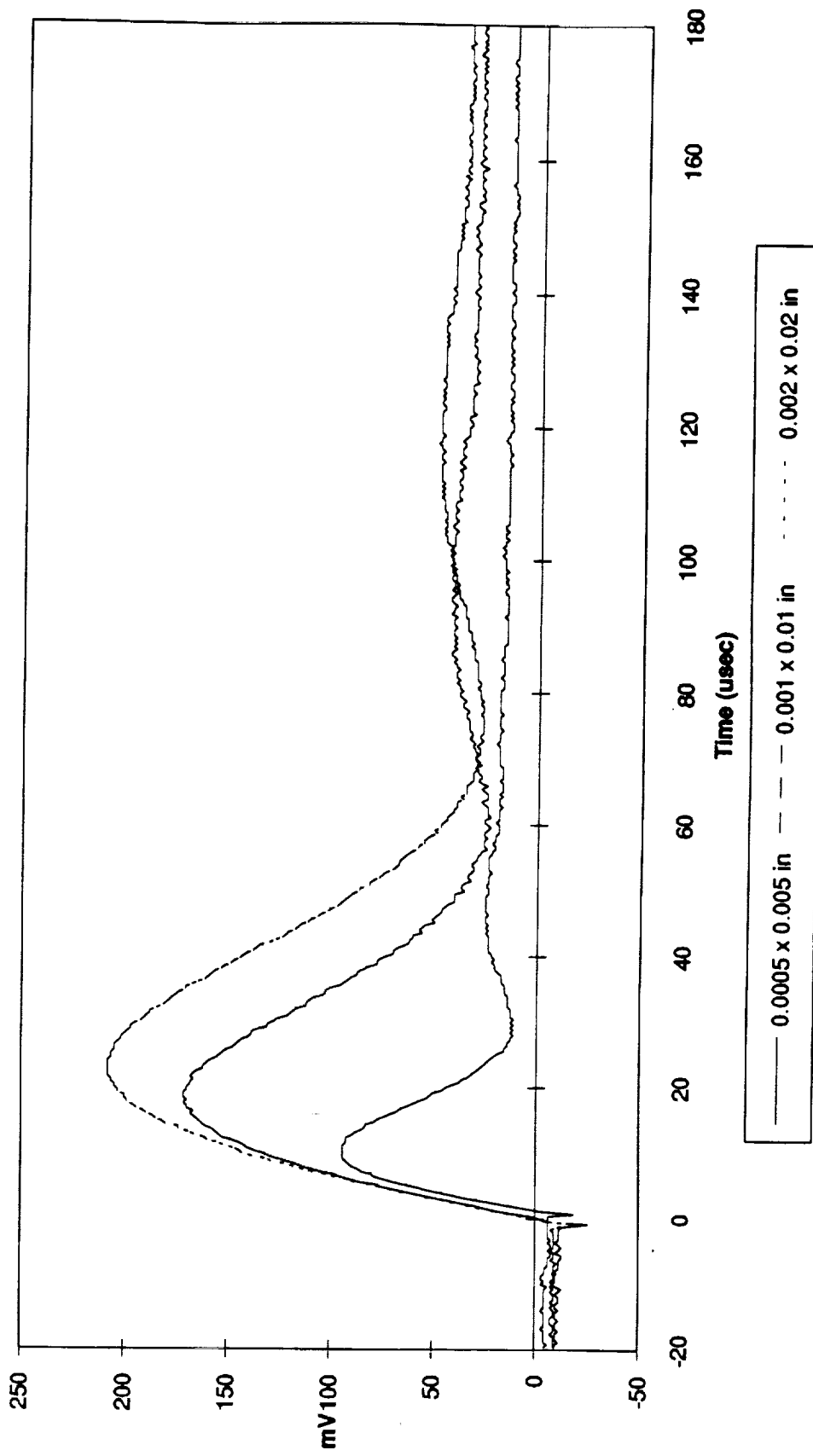


Fig 7

Normalized Anemometer I Response To Square Wave For Different Sensor Sizes (First Overheat)

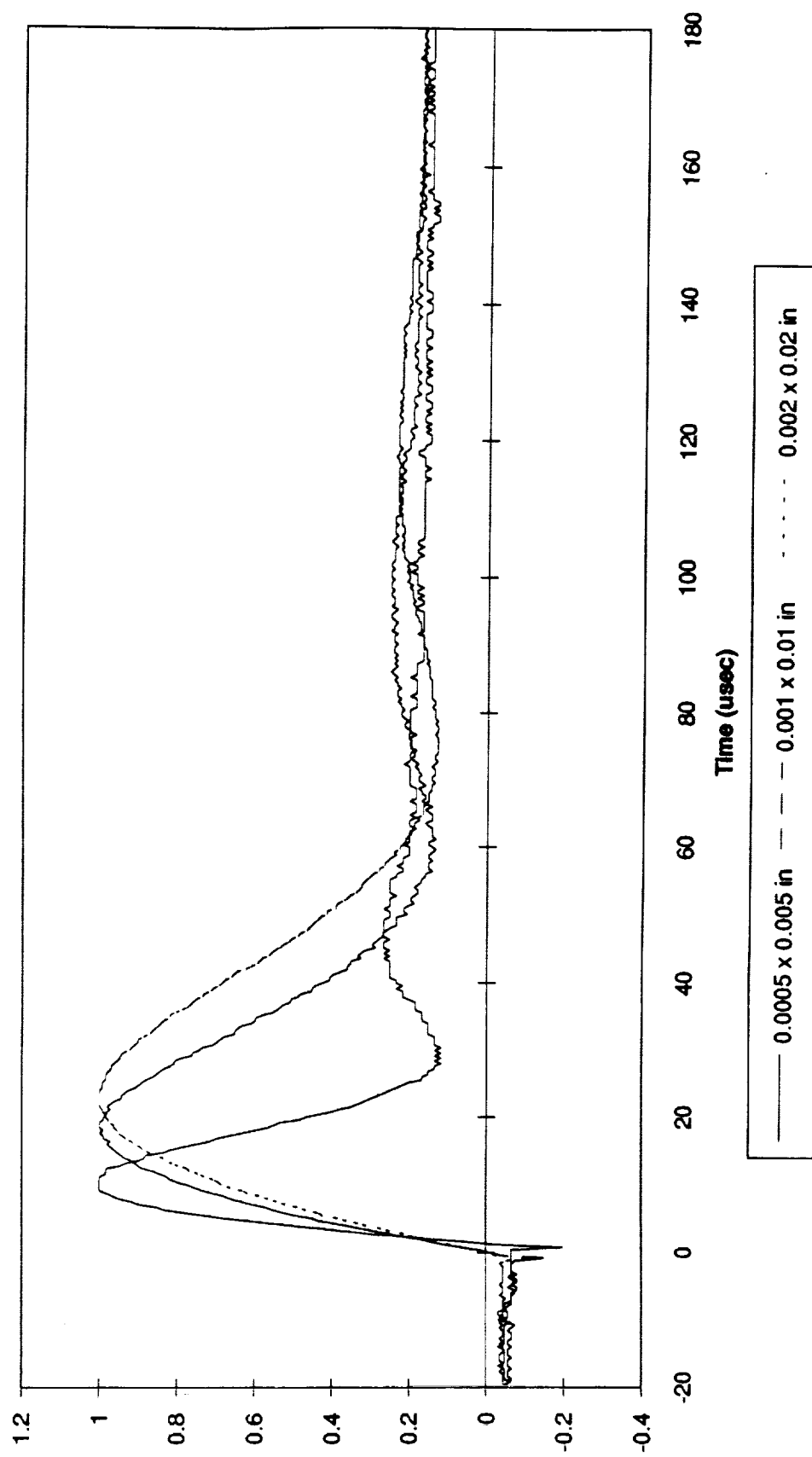
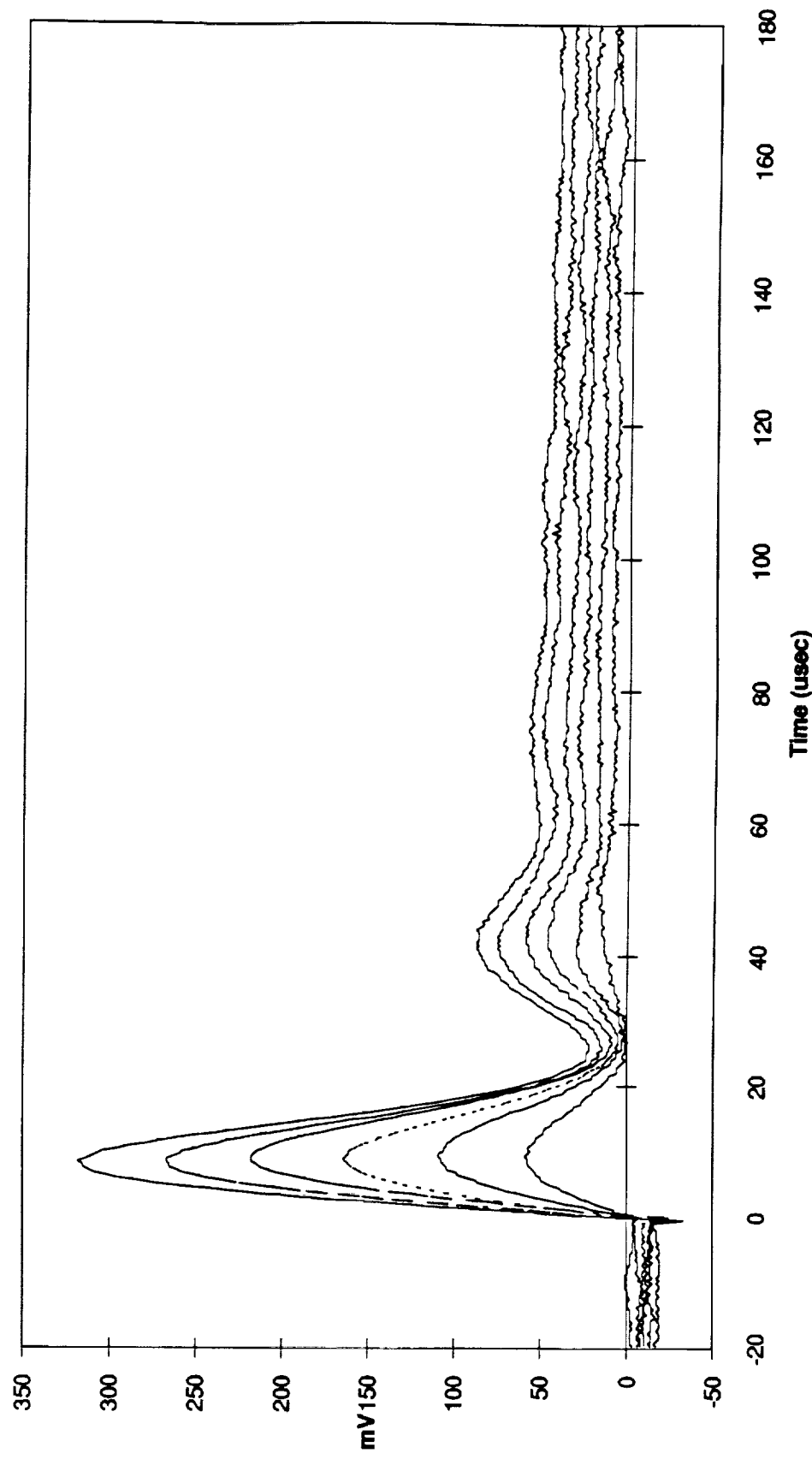


Fig. 8

Anemometer II Response To Varied Voltage Square Waves Using 0.0005 x
0.0005 Sensor At Overheat 1.19



F16 7

Anemometer II Response To Varied Voltage Square Waves Using 0.005 x
0.0005 Sensor At Overheat 1.19 (Normalized)

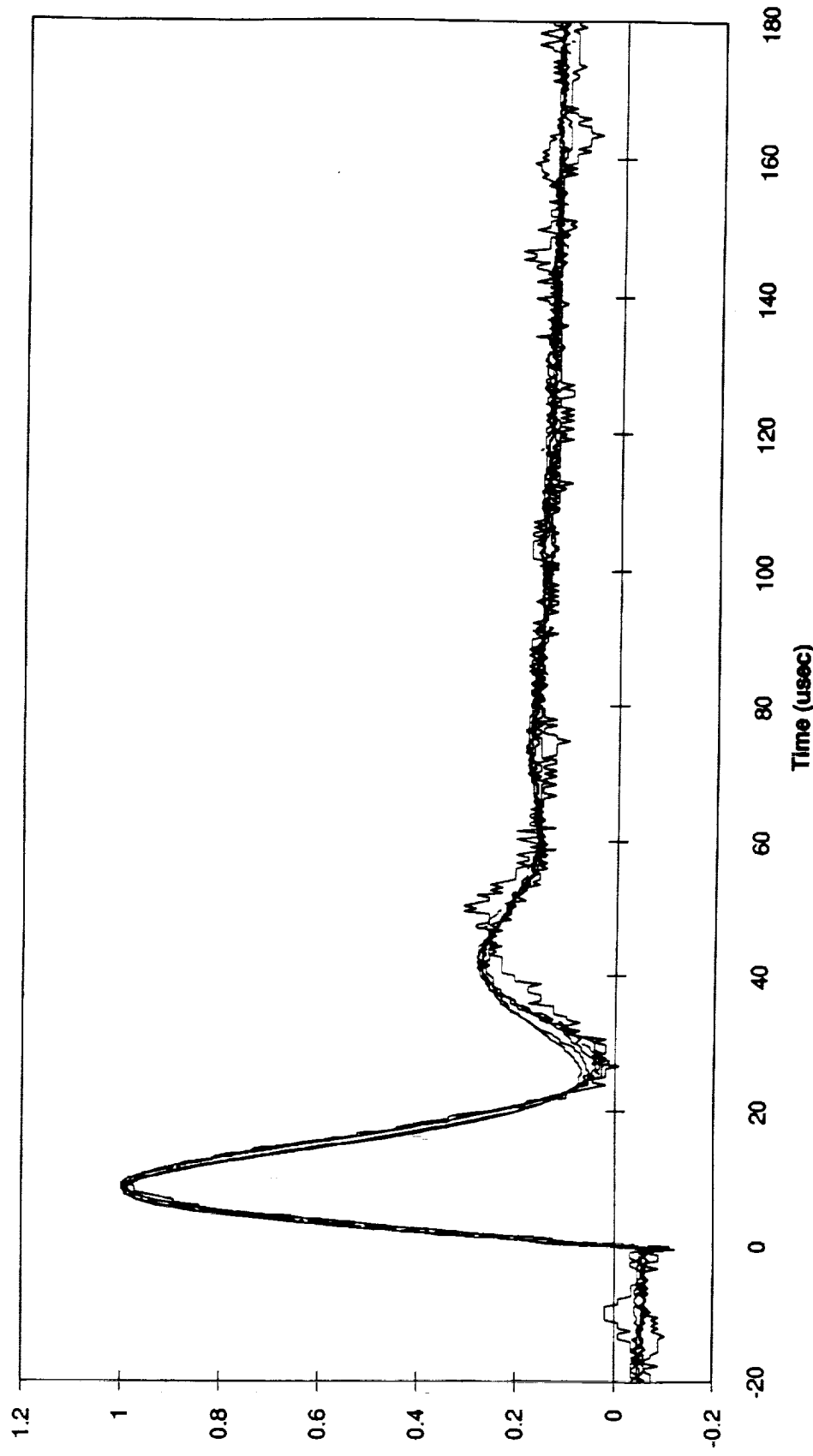


Fig. 10

**Square Wave Response Normalization Factor Anemometer II Using 0.005 x
0.0005 Sensor At Overheat 1.19**

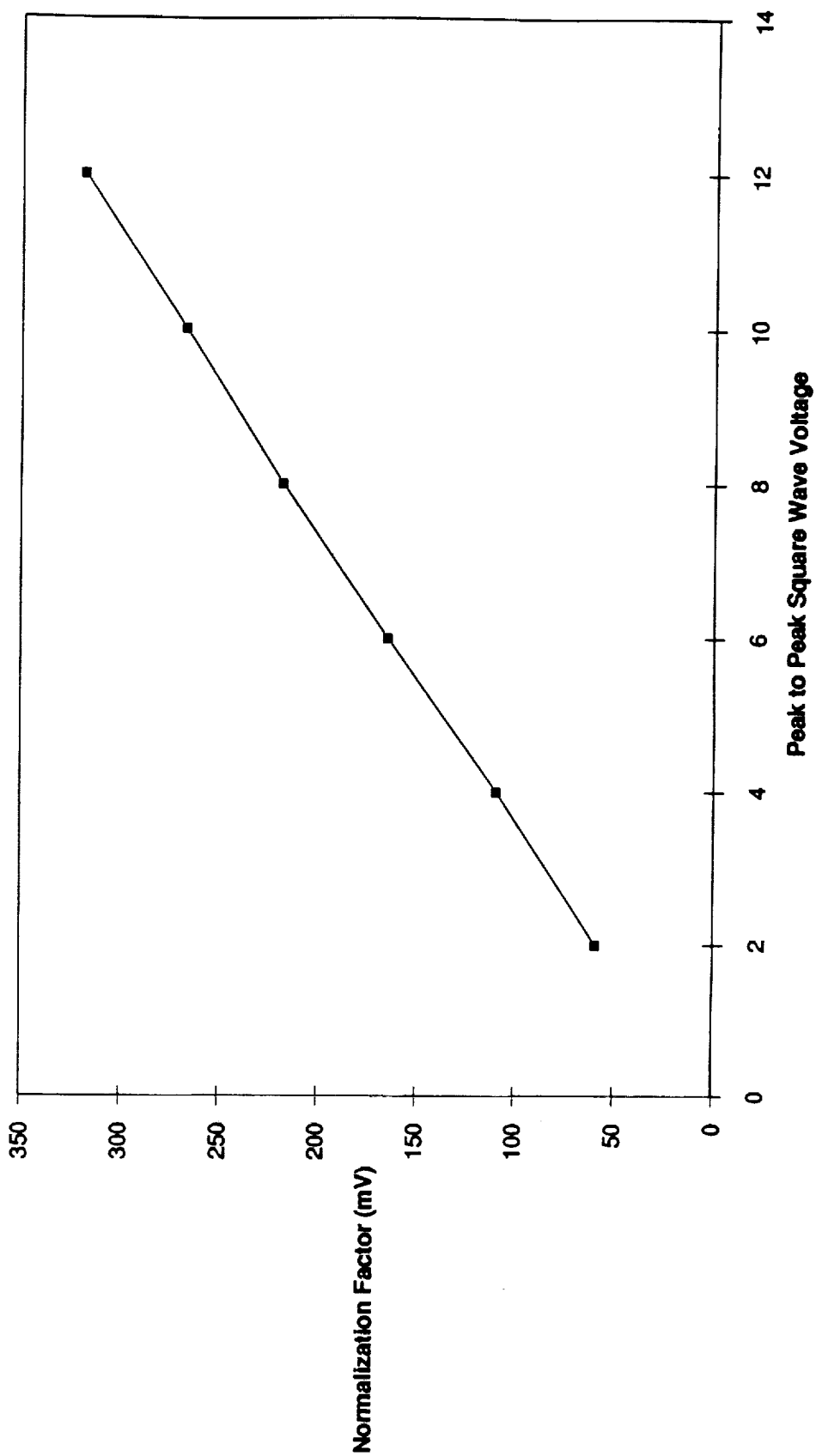


Fig 11

**Anemometer II Response To 2 Volt Square Wave For Different Sensor Sizes
(First Overheat)**

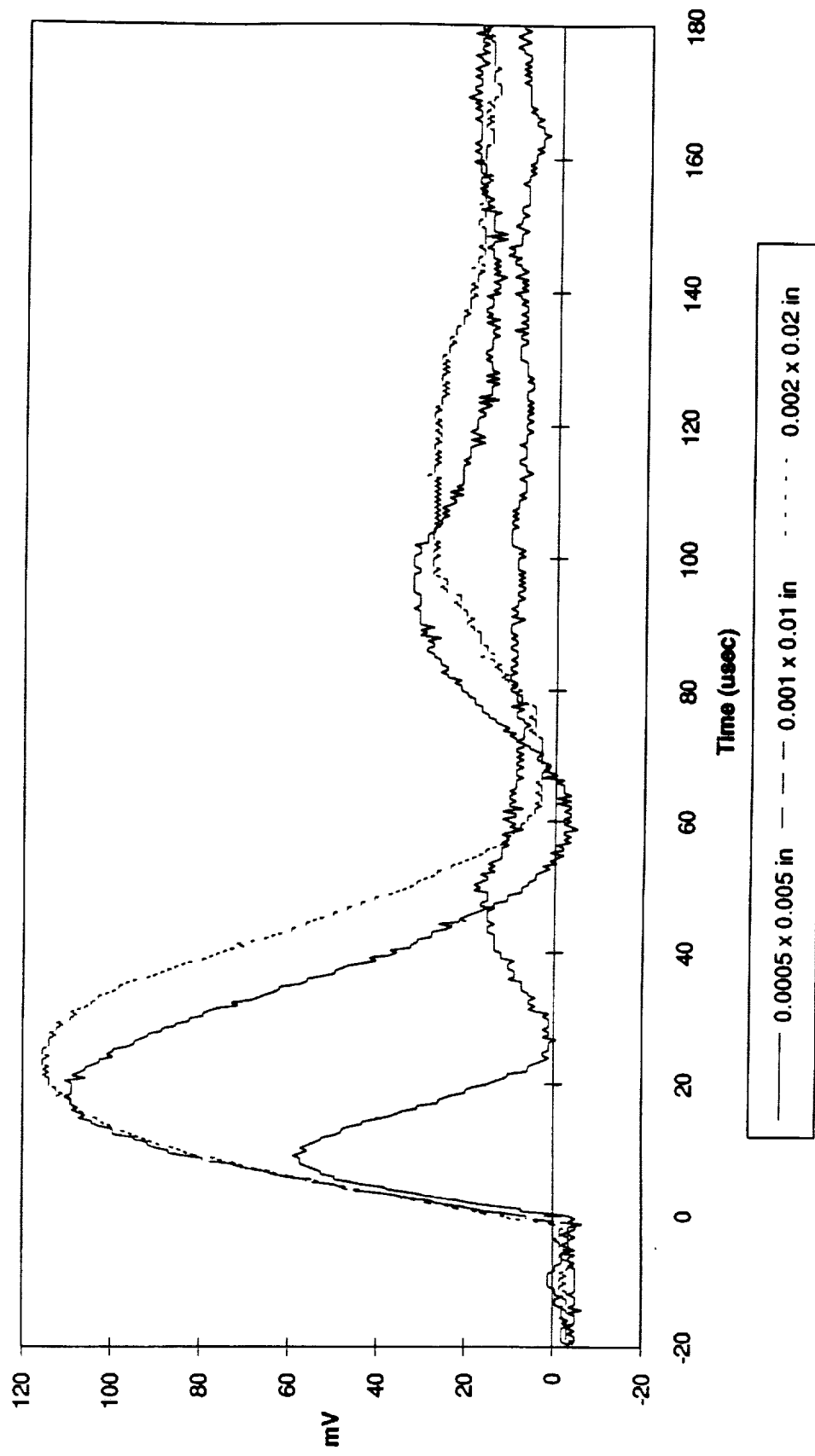


Fig. 12

**Anemometer II Response To 2 Volt Square Wave For Different Sensor Sizes
(First Overheat)**

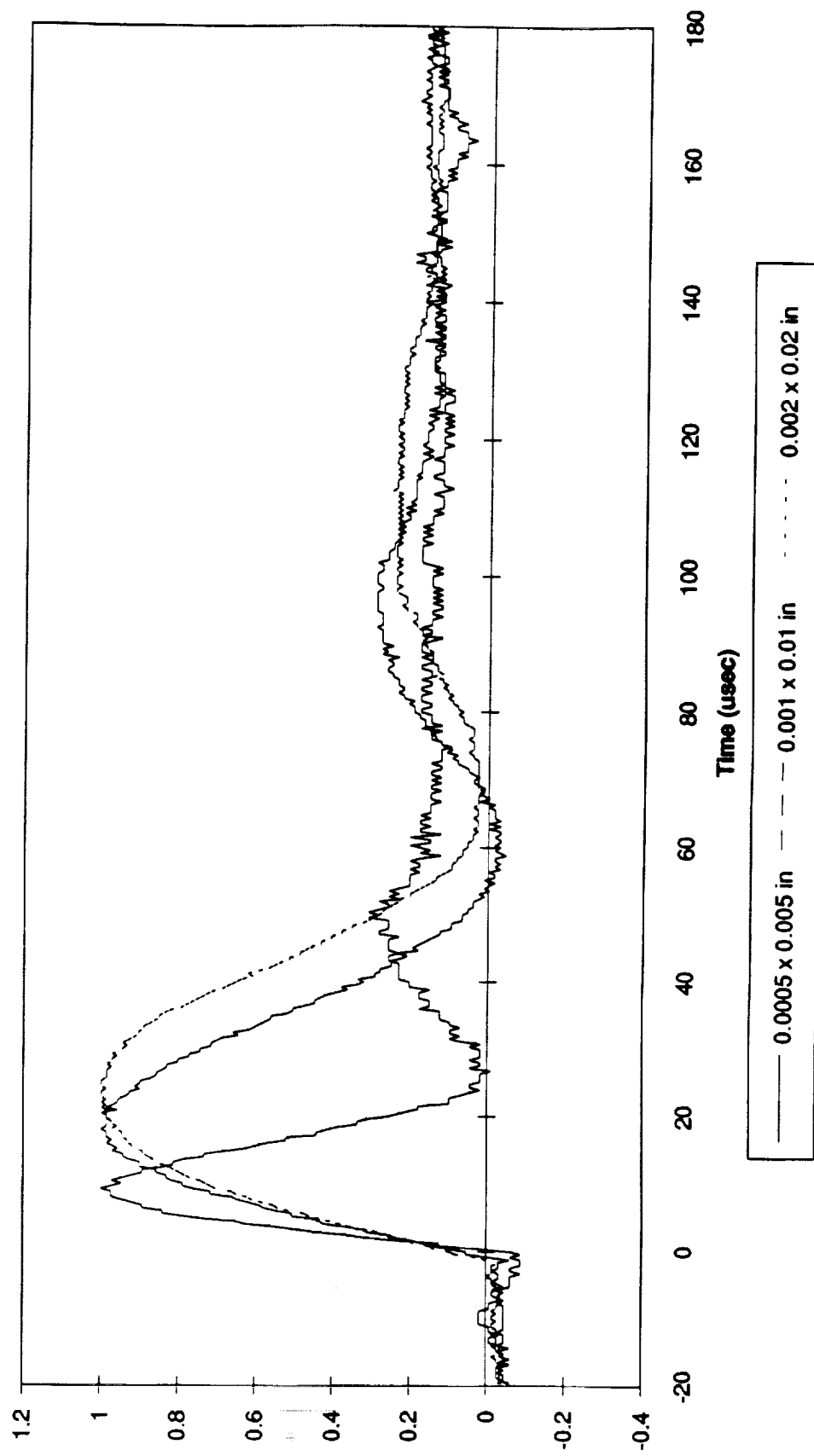
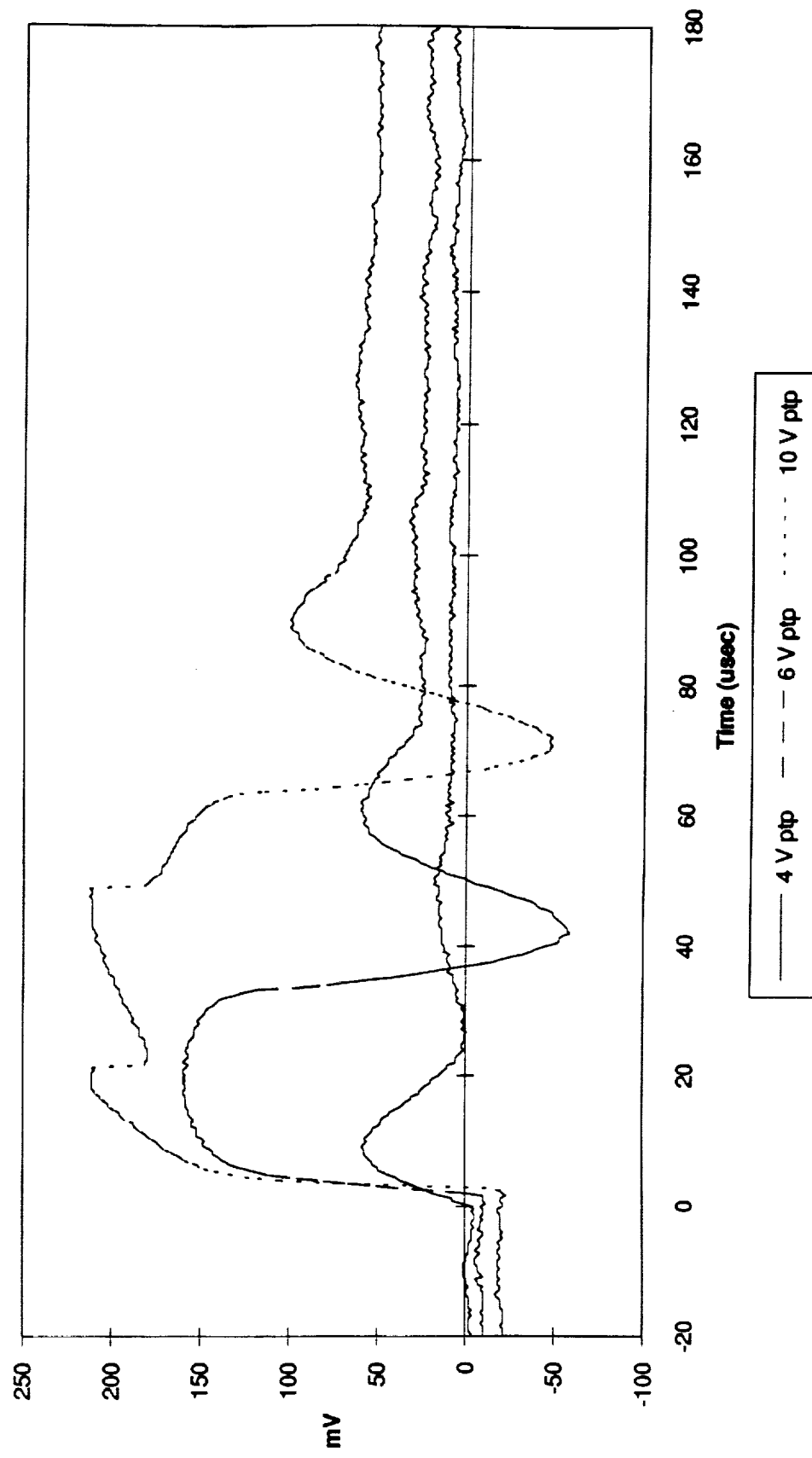


Fig 12

**Anemometer II Response To Varied Voltage Steps Using 0.02 x 0.002 Sensor
At Overheat 1.19**



Figs 14

**Anemometer I Response To Varied Voltage Square Waves Using 0.0005 x
0.0005 Sensor At Overheat 1.34**

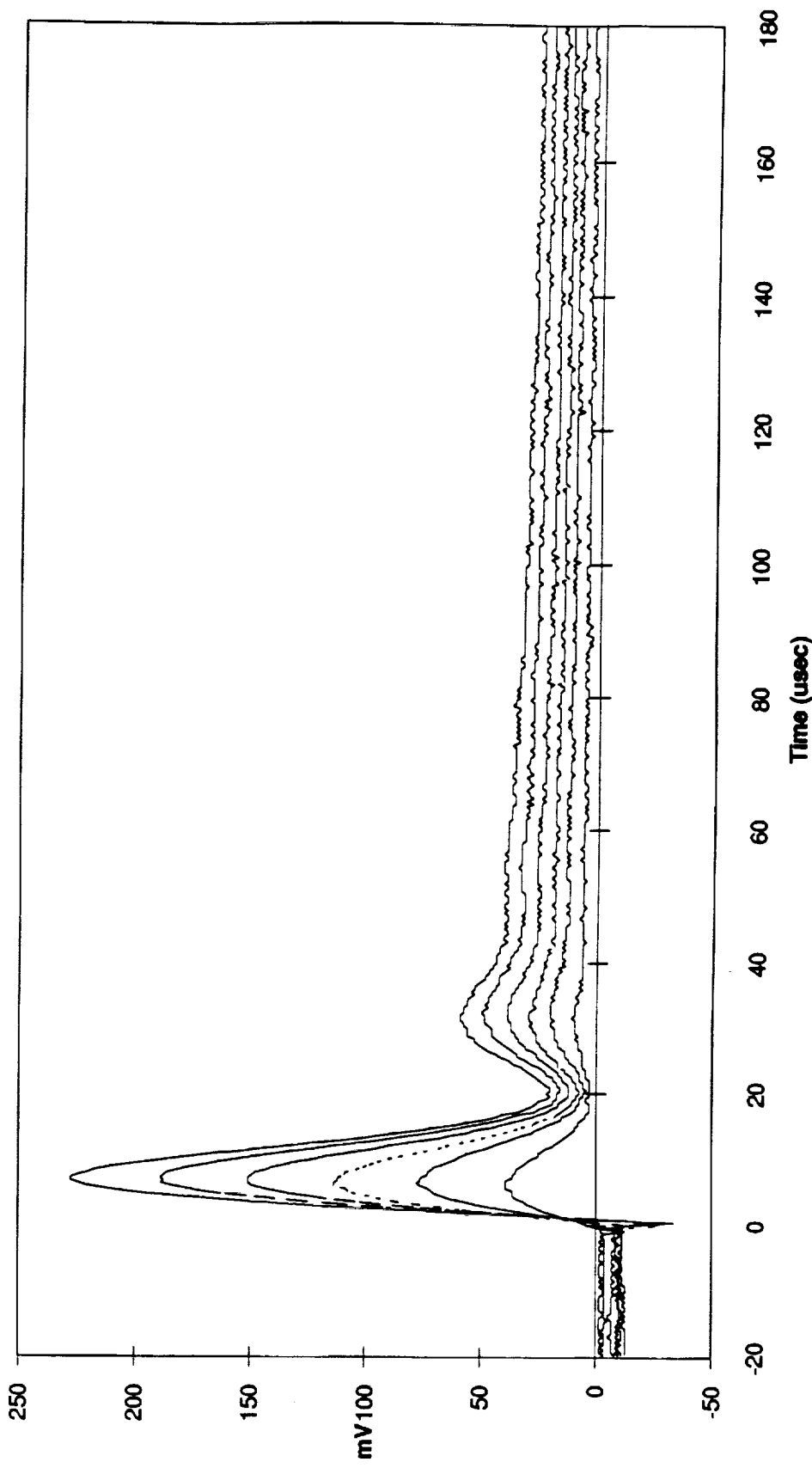


Fig 15

Anemometer I Response To Varied Voltage Square Waves Using 0.005 x
0.0005 Sensor At Overheat 1.34 (Normalized)

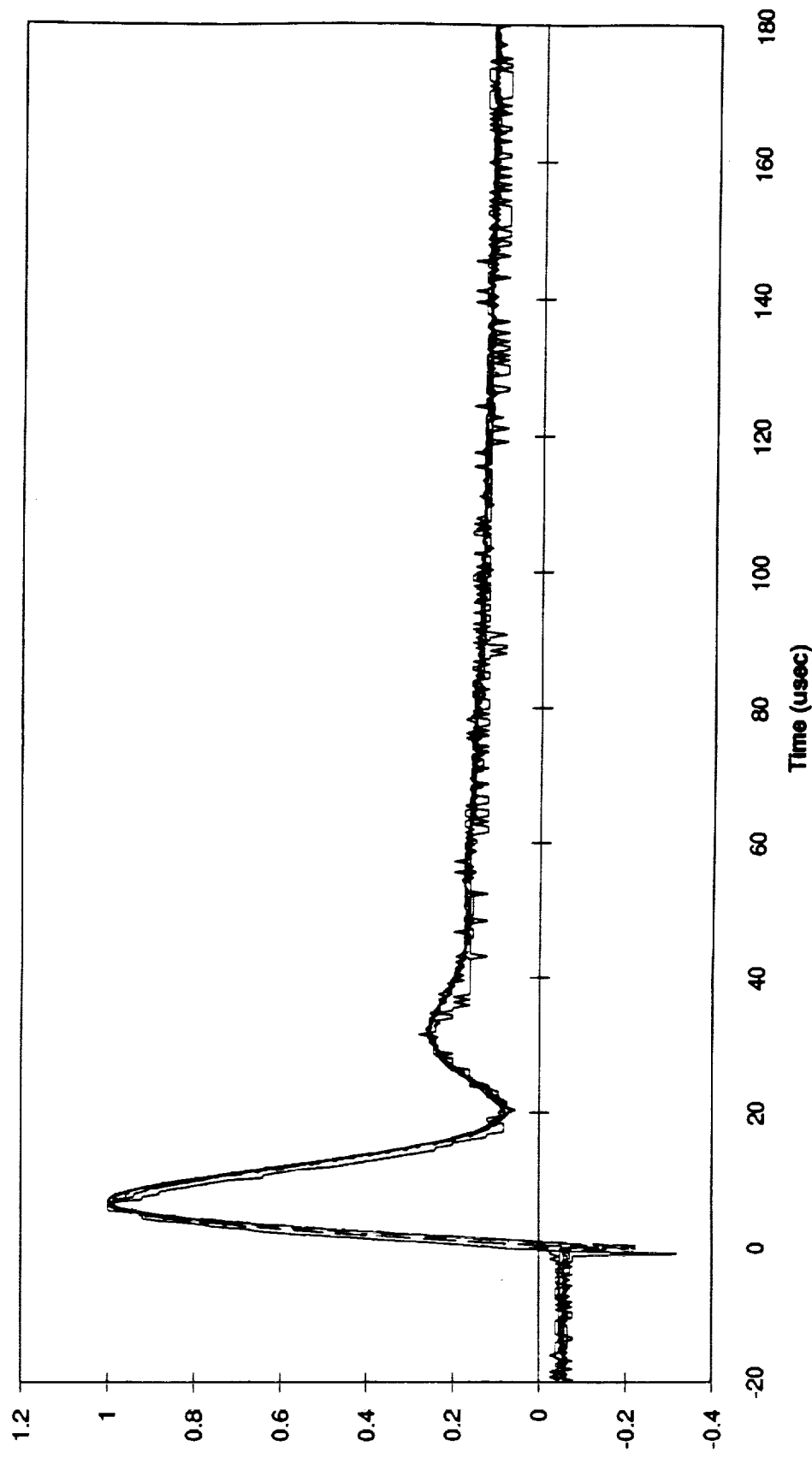


Fig 16

**Square Wave Response Normalization Factor Anemometer I Using 0.005 x
0.0005 Sensor At Overheat 1.34**

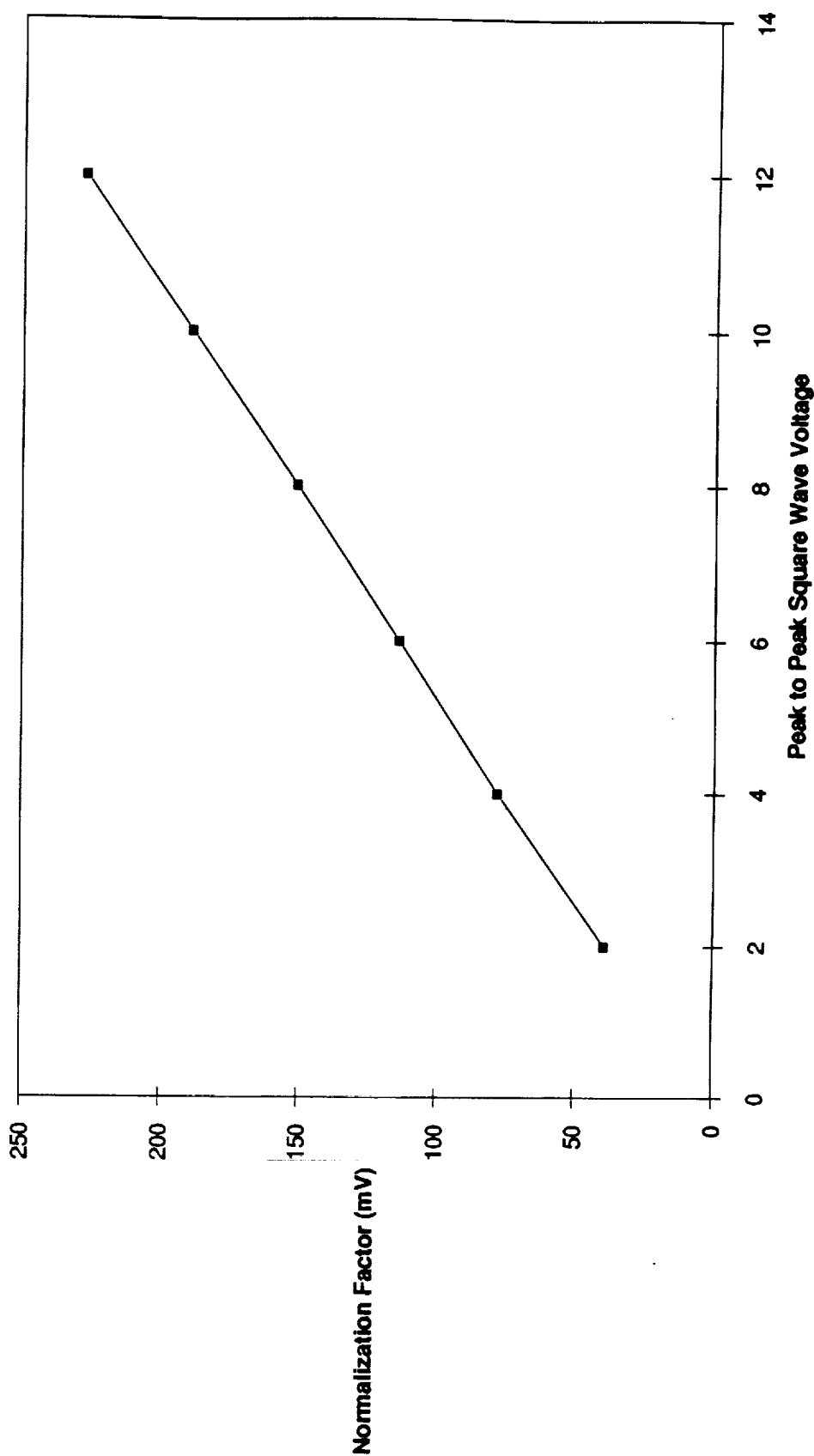
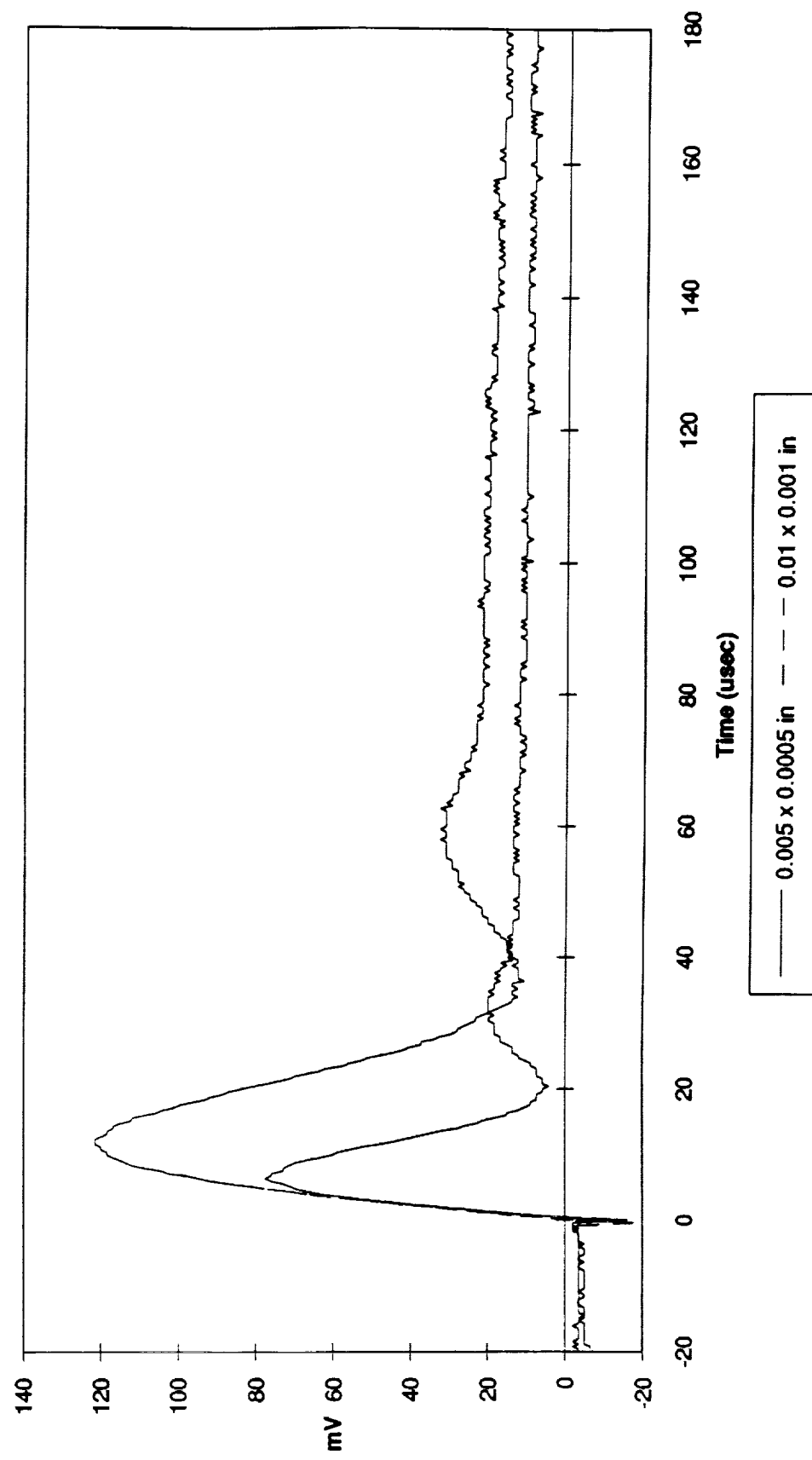


Fig 17

**Anemometer I Response To 4 Volt Square Wave For Different Sensor Sizes
(Second Overheat)**



T₁₆ 18

Normalized Anemometer I Response To Square Wave For Different Sensor Sizes (Second Overheat)

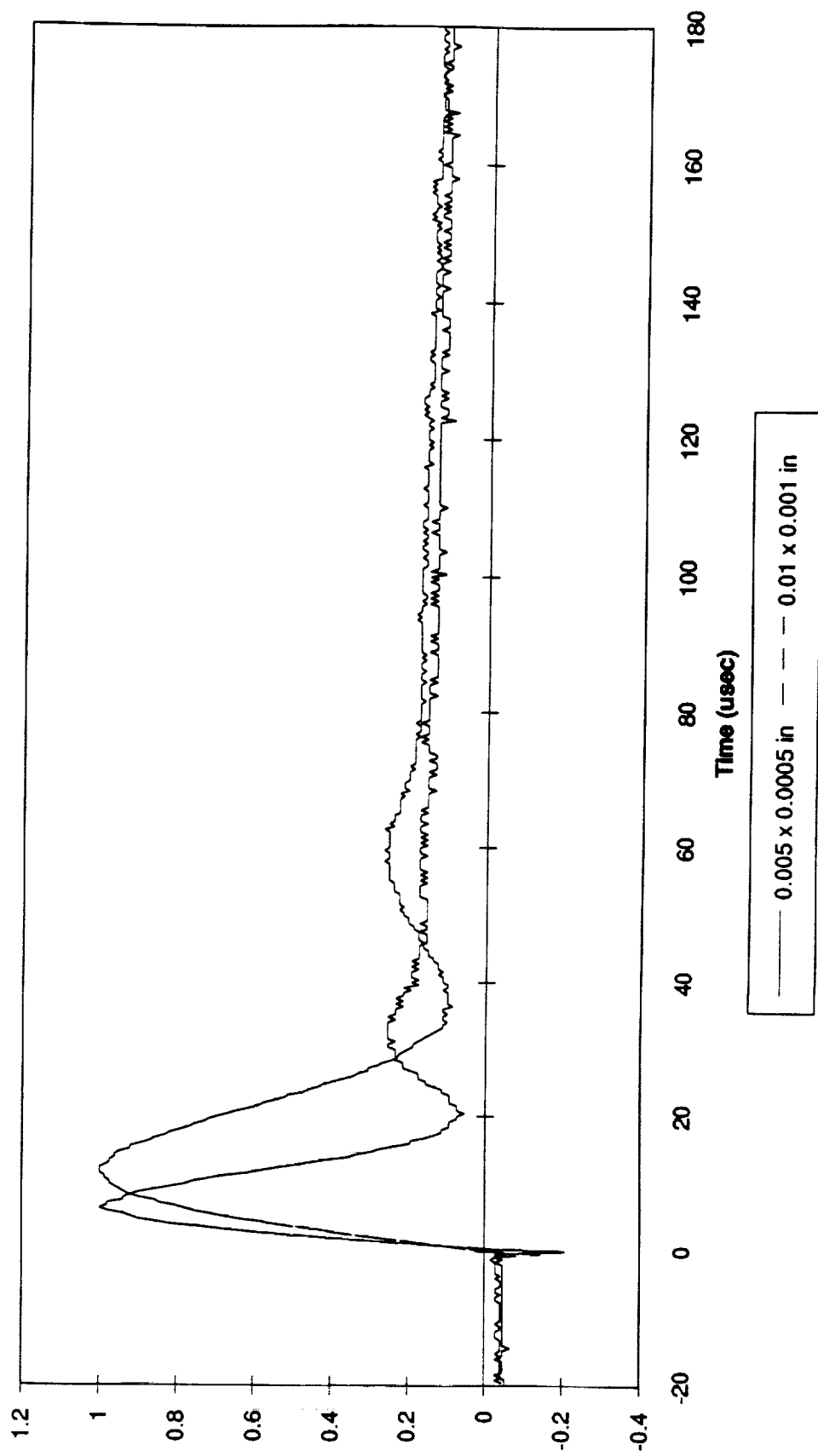
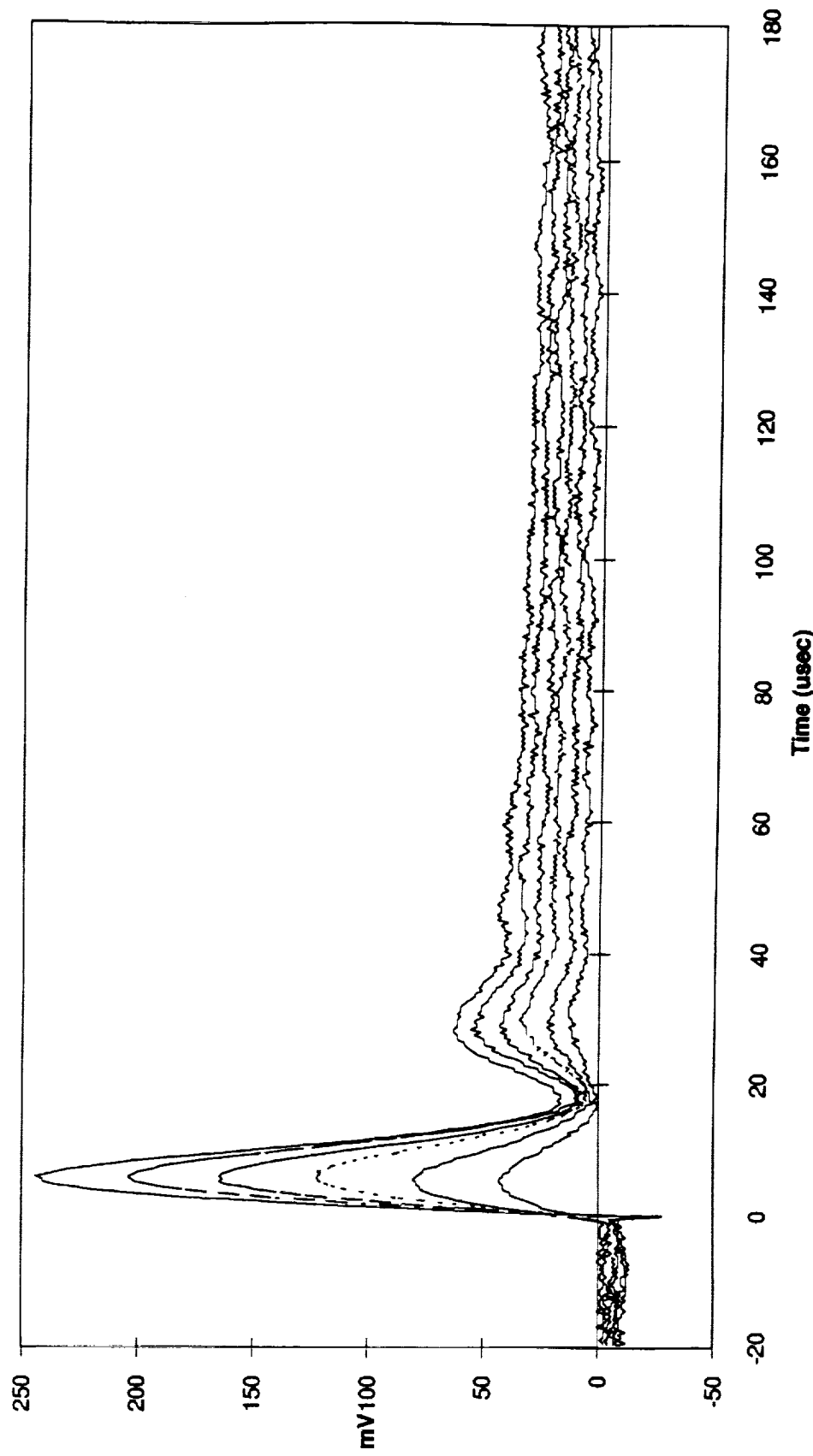


Fig 17

Anemometer II Response To Varied Voltage Square Waves Using 0.0005 x
0.0005 Sensor At Overheat 1.34



$\bar{f}_{10} = 2 C_1$

**Anemometer II Response To Varied Voltage Square Waves Using 0.005 x
0.0005 Sensor At Overheat 1.34 (Normalized)**

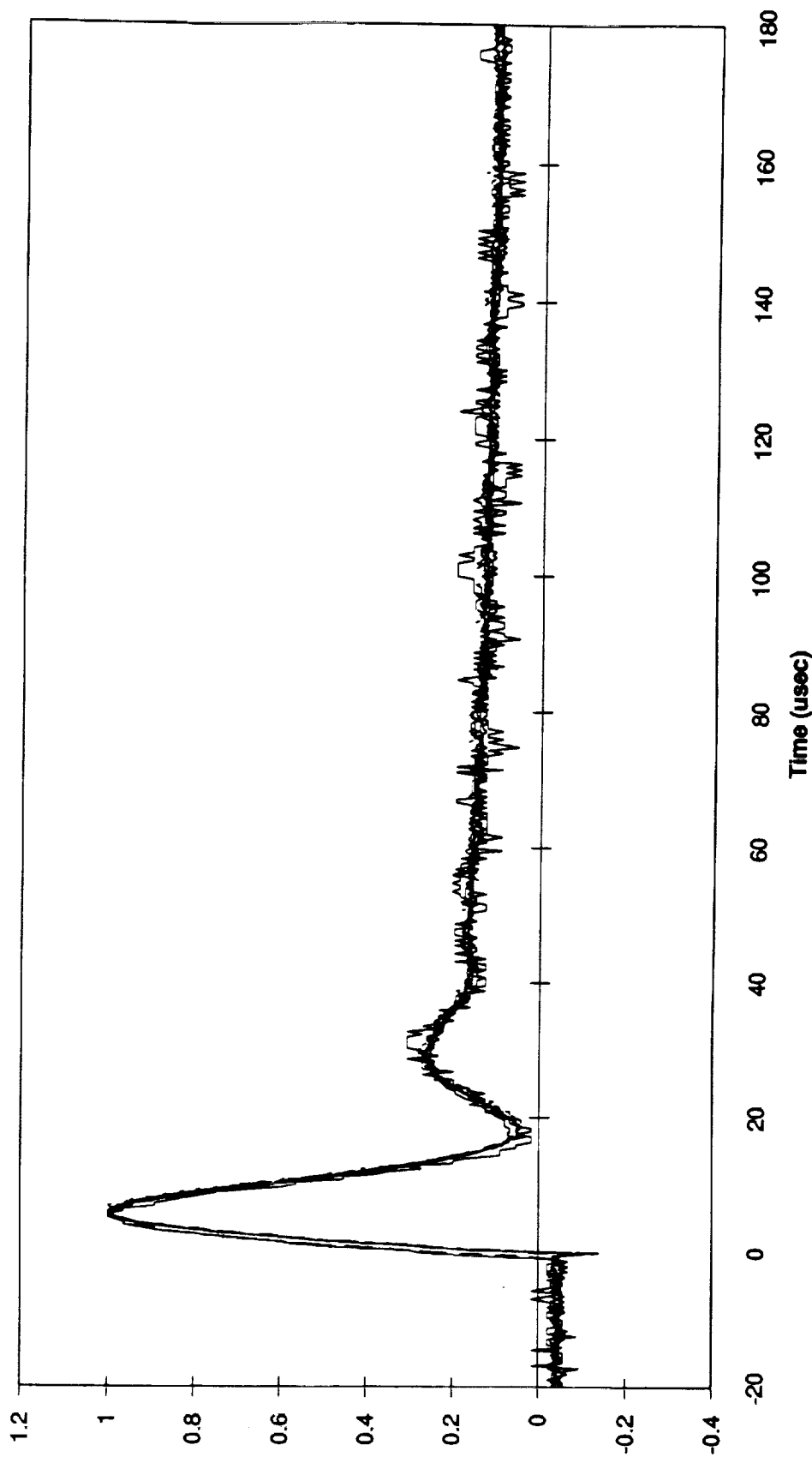


Fig 21

**Square Wave Response Normalization Factor Anemometer II Using 0.005 x
0.0005 Sensor At Overheat 1.34**

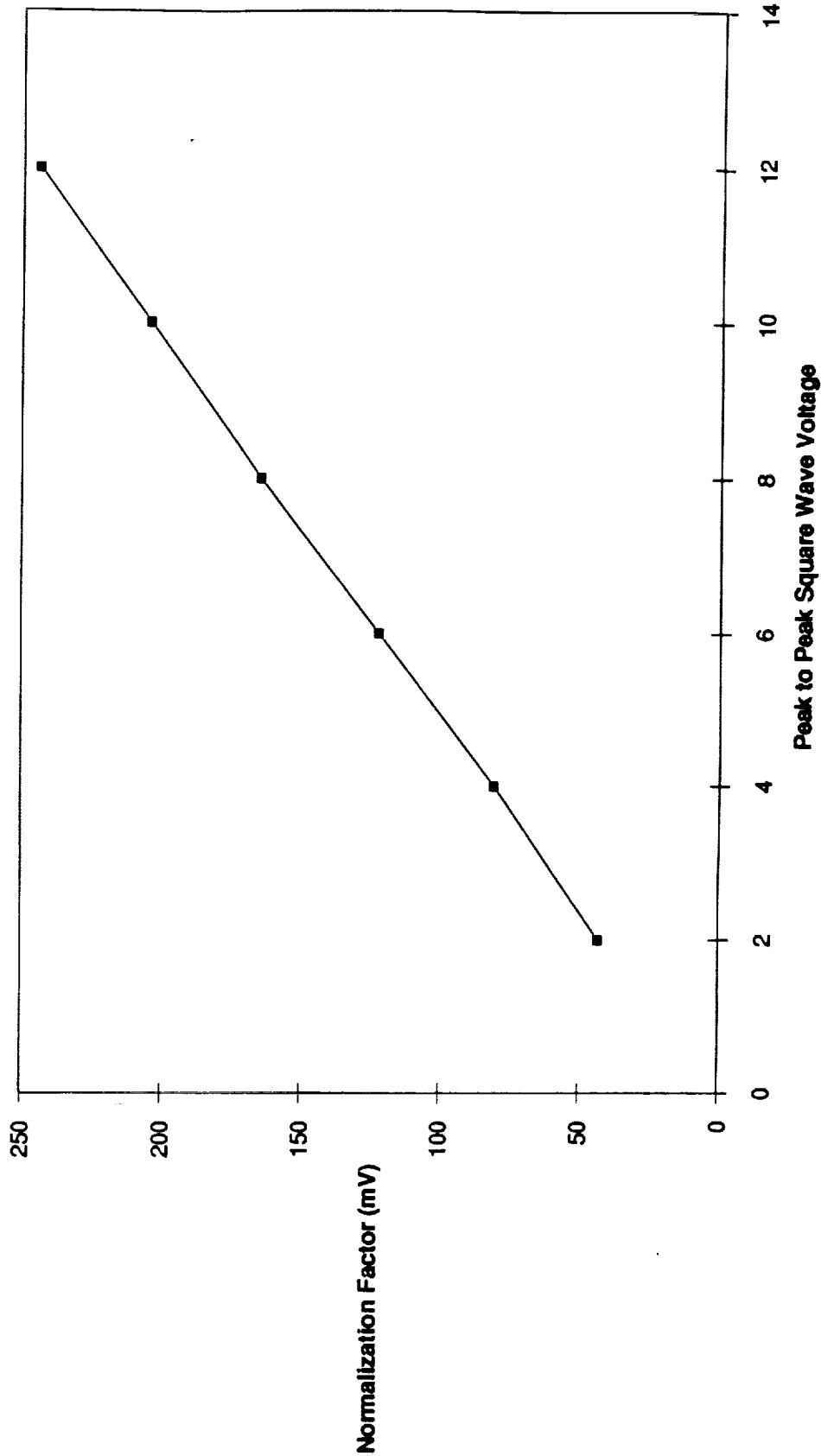


Fig. 22

**Anemometer II Response To 4 Volt Square Wave For Different Sensor Sizes
(Second Overheat)**

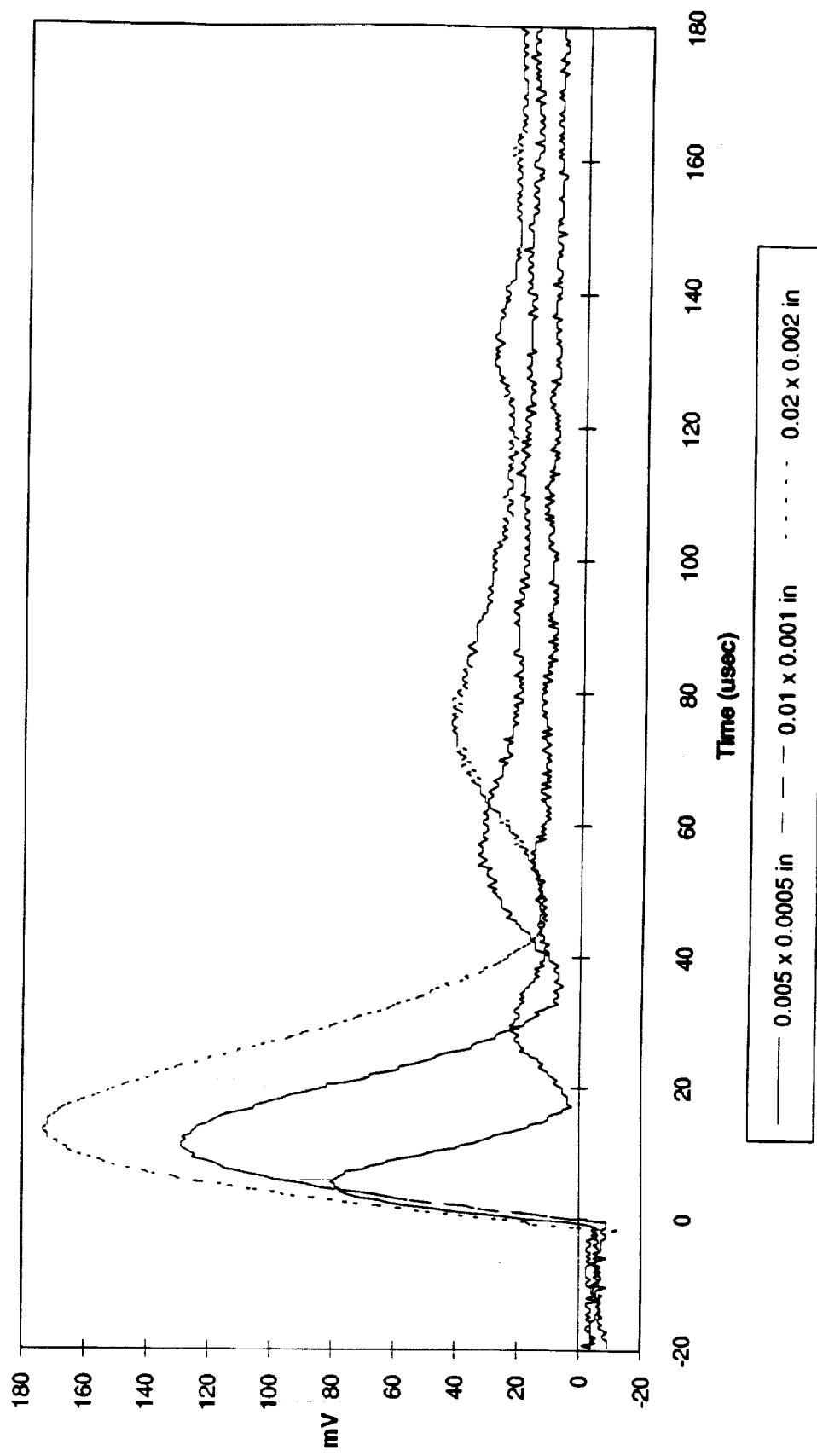


Fig 23

Normalized Anemometer II Response To Square Wave For Different Sensor Sizes (Second Overheat)

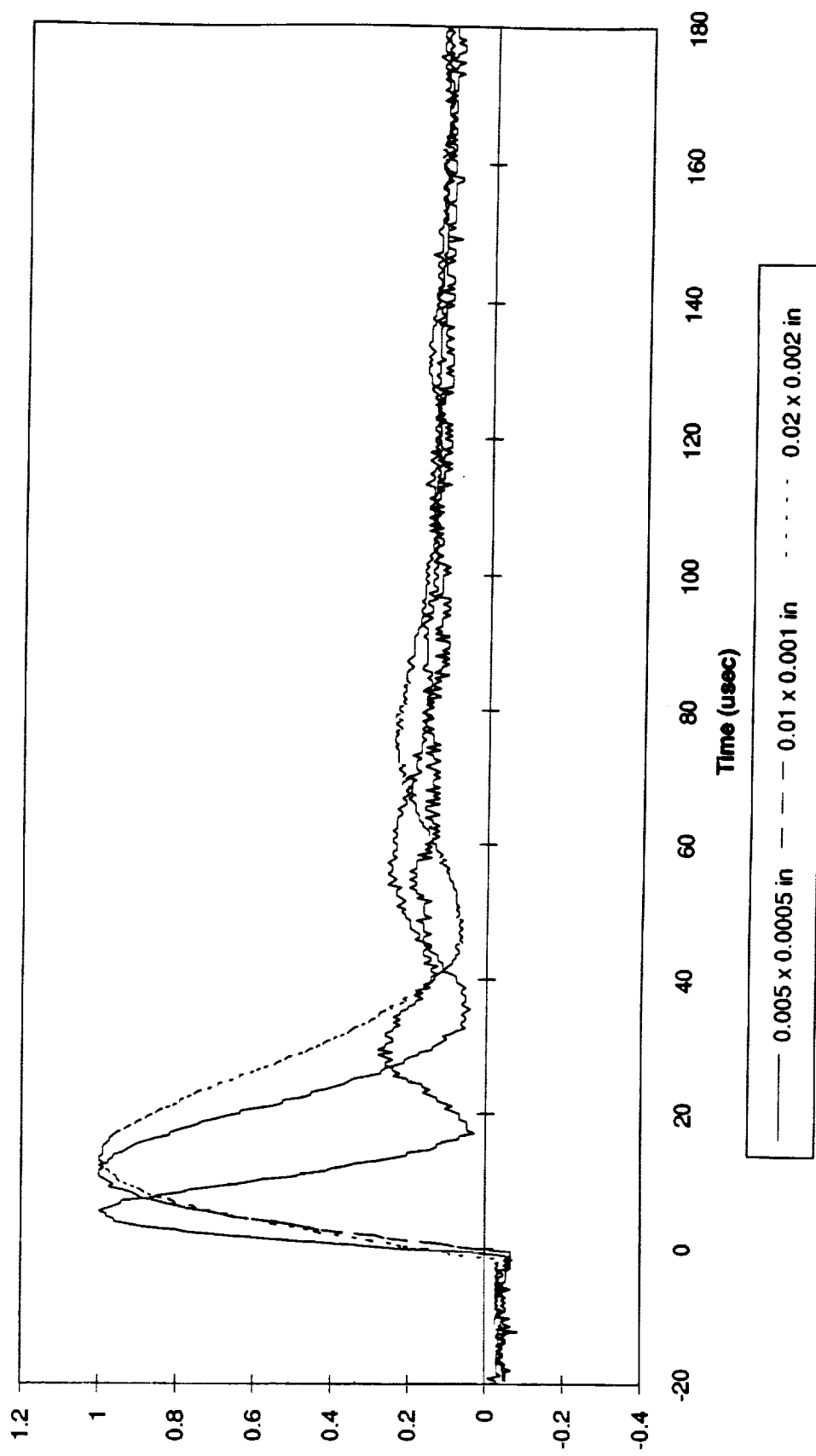


FIG 24

Normalized Anemometer II Response To Square Wave For Different Sensor Sizes (Third Overheat)

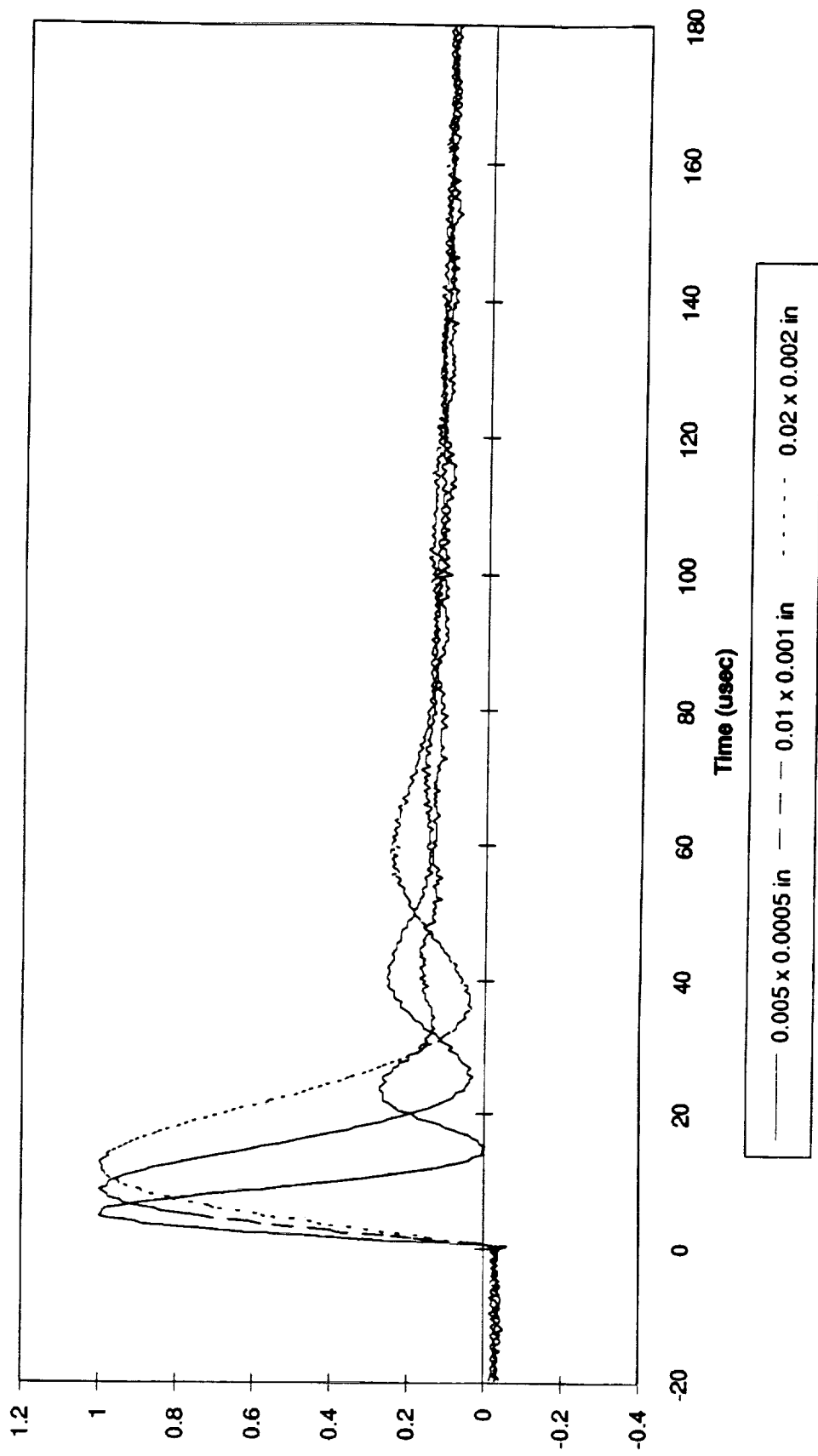


Fig. 25

Normalized Anemometer II Response To Square Wave For Different Sensor Sizes (Fourth Overheat)

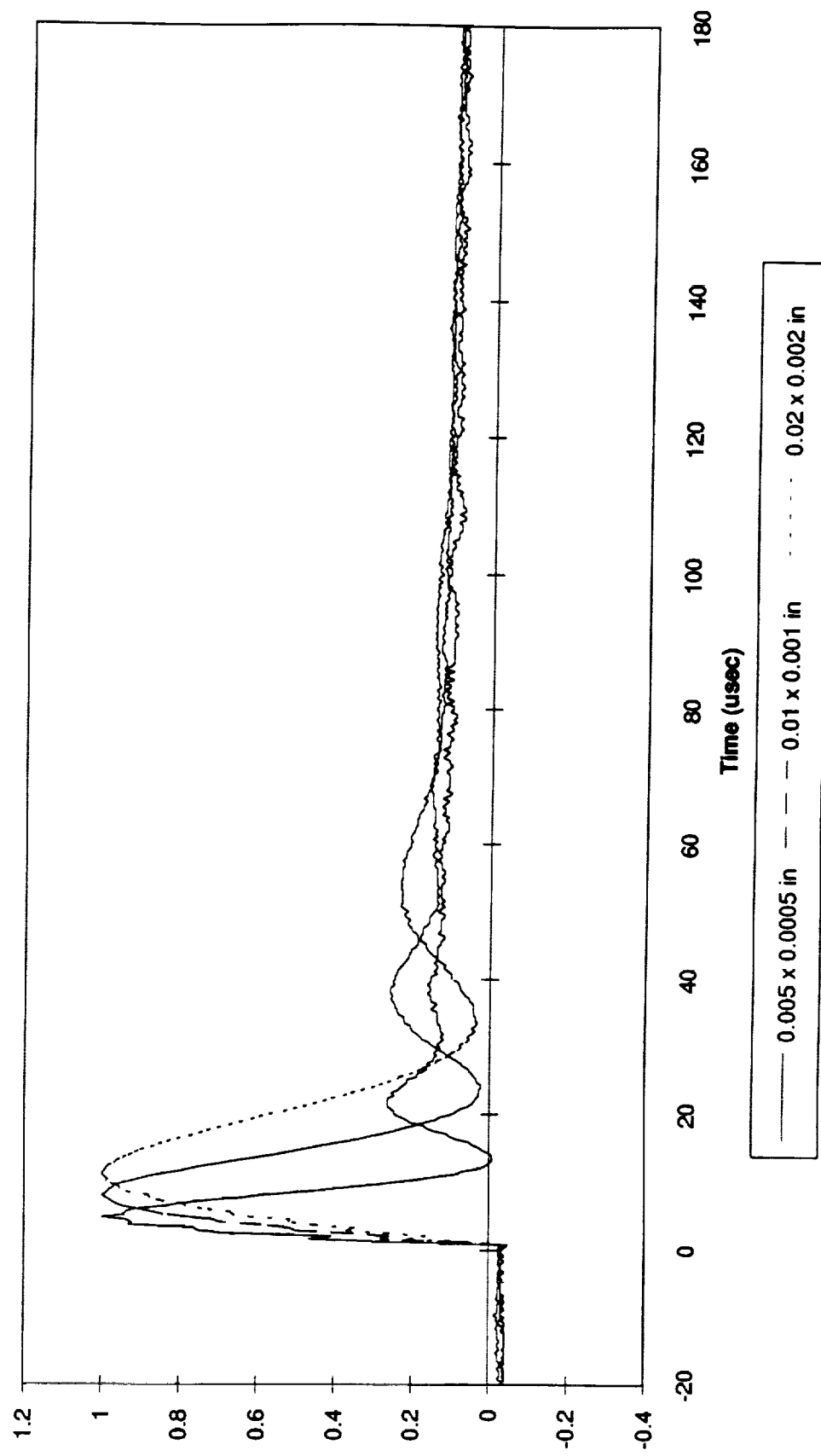
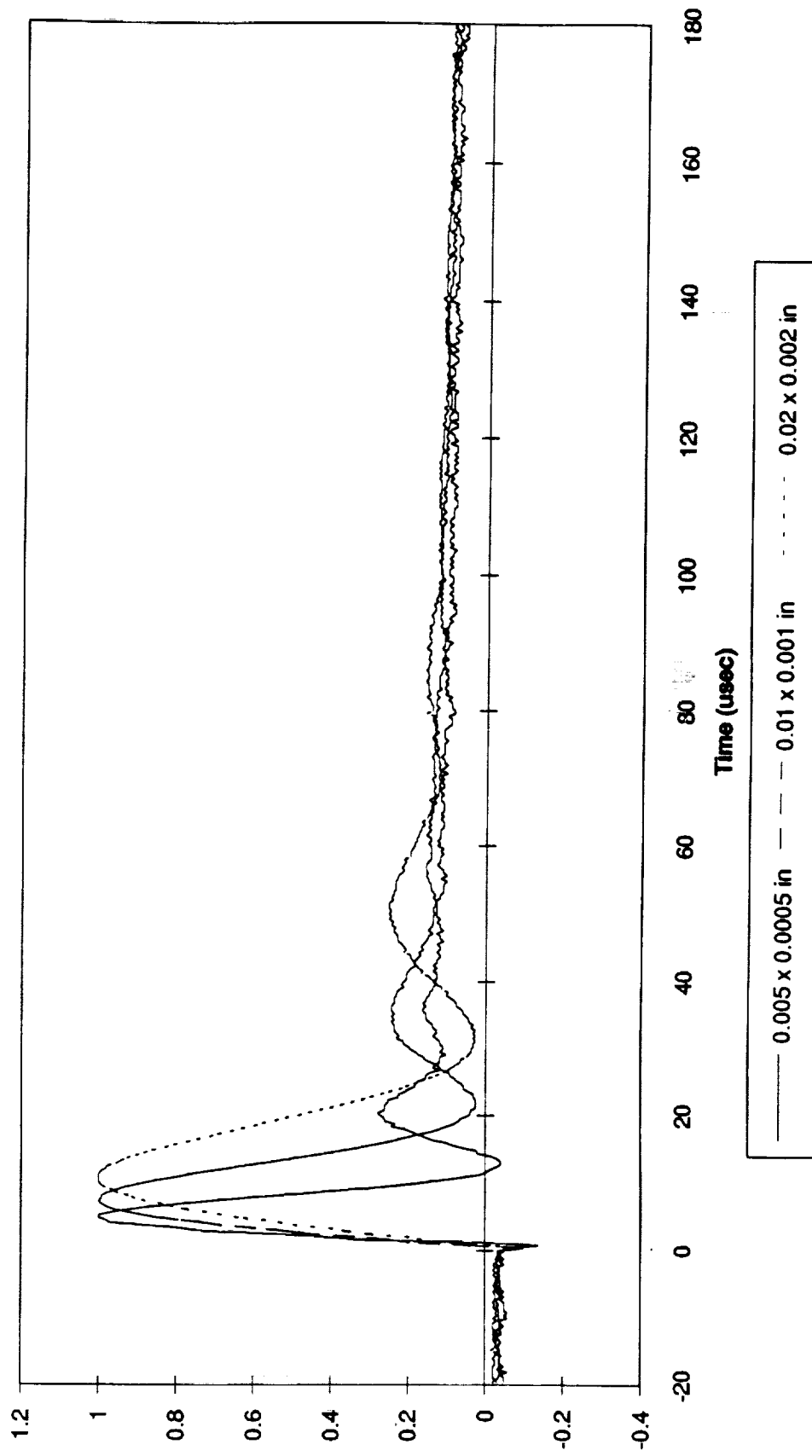


Fig 26

Normalized Anemometer II Response To Square Wave For Different Sensor Sizes (Fifth Overheat)



**Normalized Anemometer II Response With 0.005×0.0005 in Sensor To
Square Wave For Different Overheats**

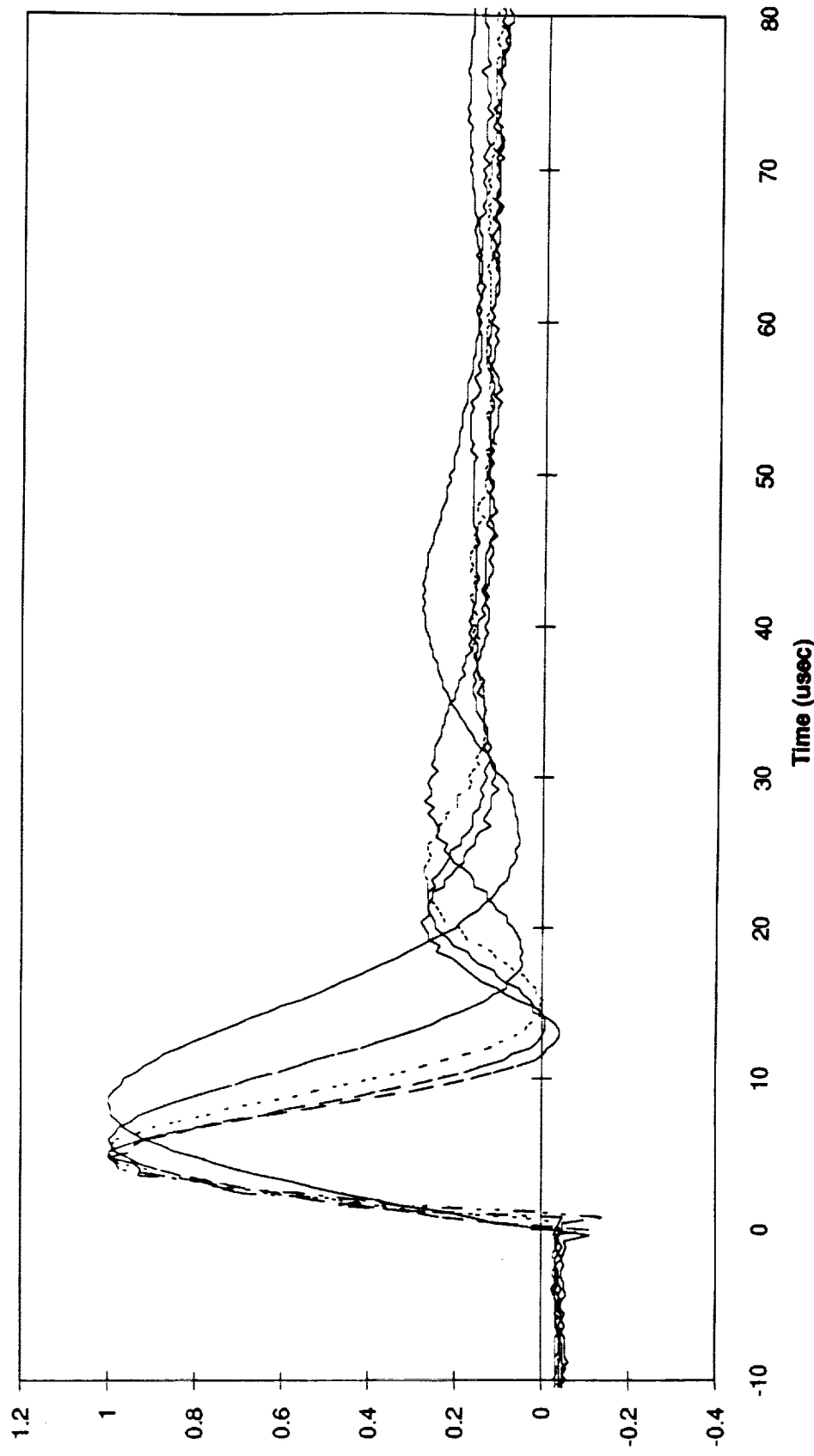
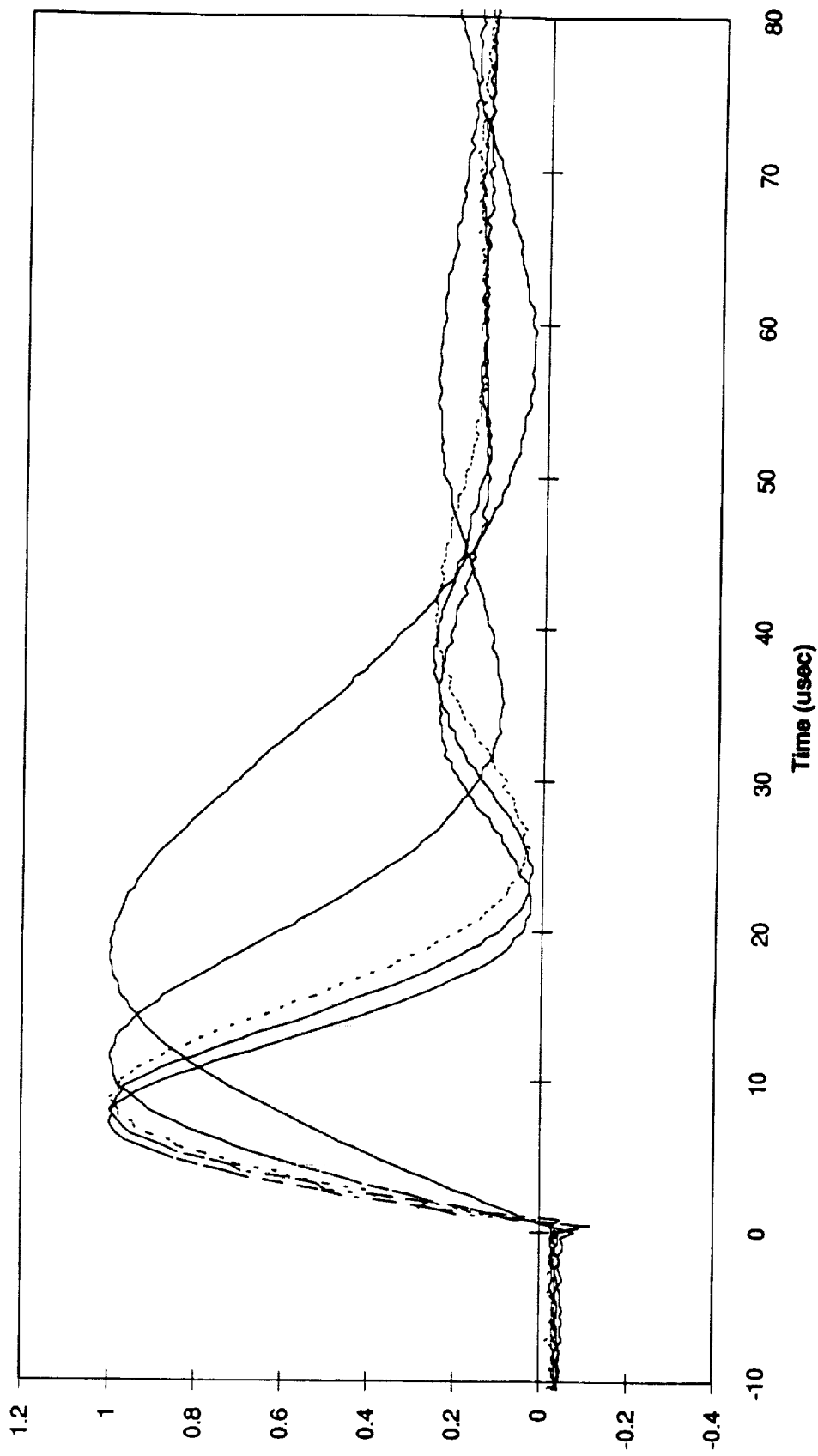


Fig 28

Normalized Anemometer II Response With 0.01×0.001 in Sensor To Square Wave For Different Overheats



$\bar{F}_{1,0} z^{\alpha}$

Normalized Anemometer II Response With 0.02×0.002 in Sensor To Square Wave For Different Overheats

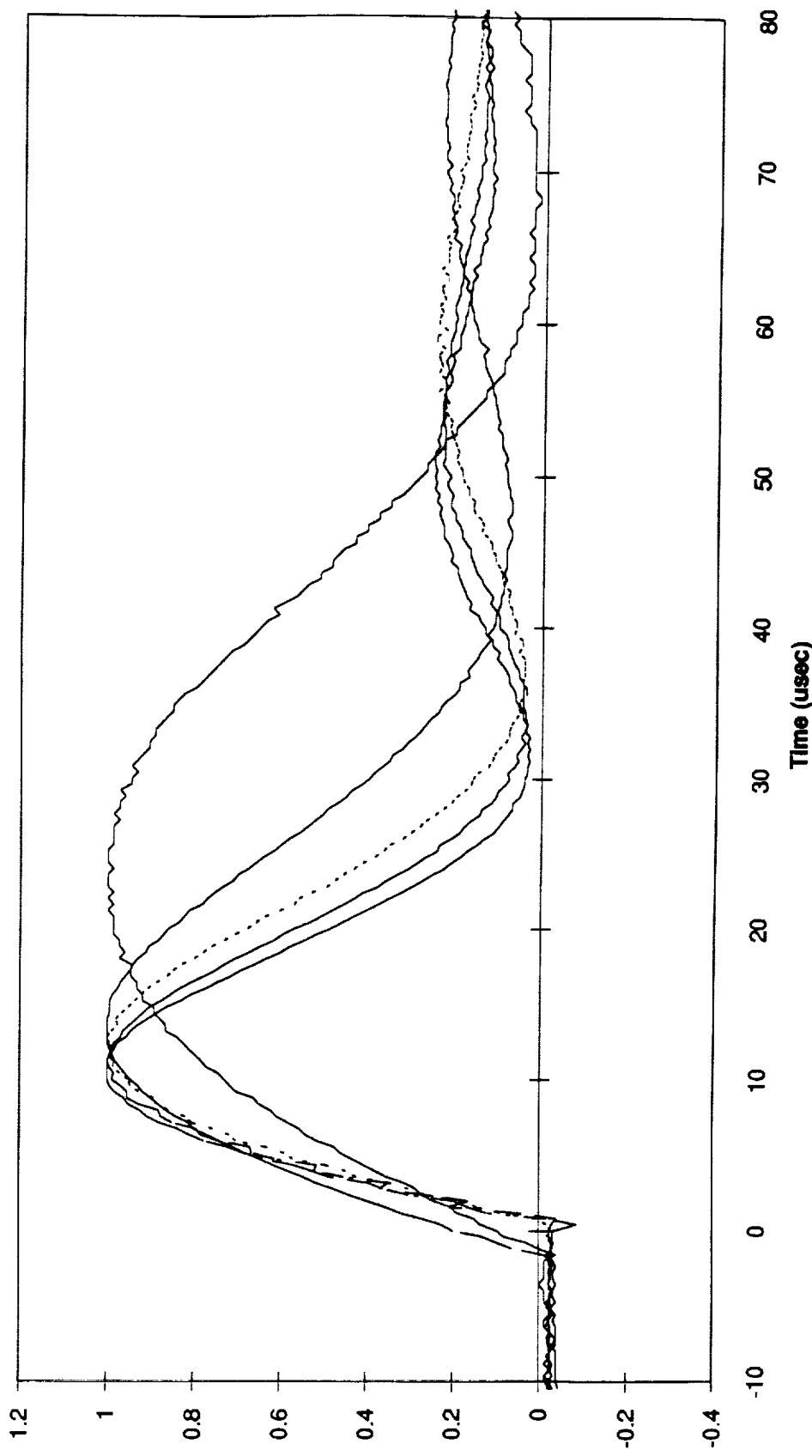


Fig 3C

Table 1

Anemometer I				
Sensor 0.005 x 0.0005				
Case	Overheat	Response	Frequency	
1	1.194	28.4	35.211	
2	1.343	19.8	50.505	
3				
4				
5				

Anemometer II				
Sensor 0.005 x 0.0005				
Case	Overheat	Response	Frequency	
1	1.194	26.4	37.879	
2	1.343	18.0	55.556	
3	1.512	14.4	69.444	
4	1.593	12.4	80.645	
5	1.700	12.0	83.333	

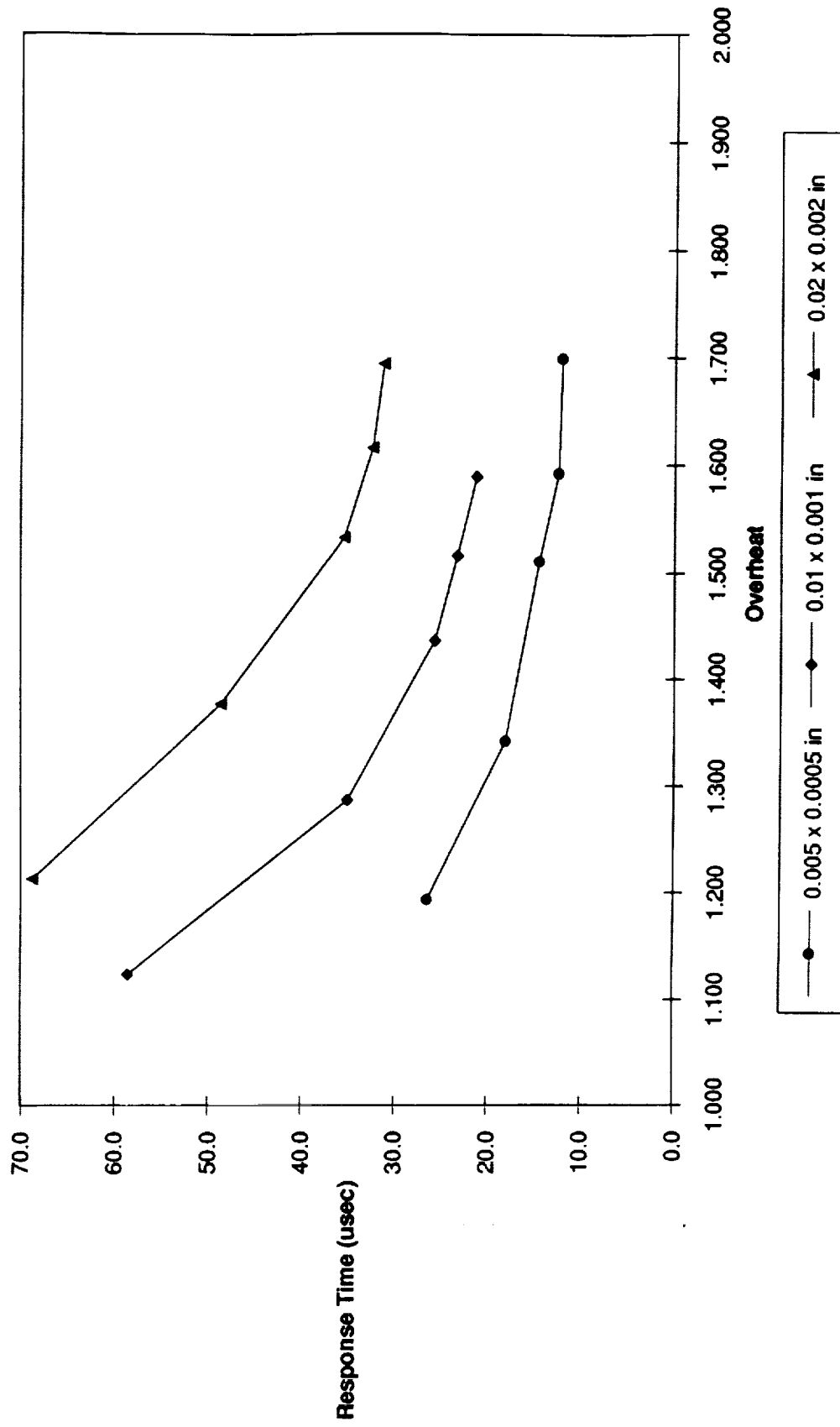
Anemometer I				
Sensor 0.01 x 0.001				
Case	Overheat	Response	Frequency	
1	1.135	60.1	16.639	
2	1.287	37.0	27.027	
3				
4				
5				

Anemometer II				
Sensor 0.01 x 0.001				
Case	Overheat	Response	Frequency	
1	1.124	58.6	17.065	
2	1.287	35.0	28.571	
3	1.437	25.6	39.063	
4	1.517	23.2	43.103	
5	1.590	21.2	47.170	

Anemometer I				
Sensor 0.02 x 0.002				
Case	Overheat	Response	Frequency	
1	1.208	76.2	13.123	
2				
3				
4				
5				

Anemometer II				
Sensor 0.02 x 0.002				
Case	Overheat	Response	Frequency	
1	1.213	68.8	14.535	
2	1.376	48.6	20.576	
3	1.534	35.4	28.249	
4	1.616	32.4	30.864	
5	1.694	31.2	32.051	

Effects Of Increasing Overheat On Sensor Response Time (Anemometer II)



F16 31

**Effects Of Increasing Overheat On Sensor Frequency Response
(Anemometer II)**

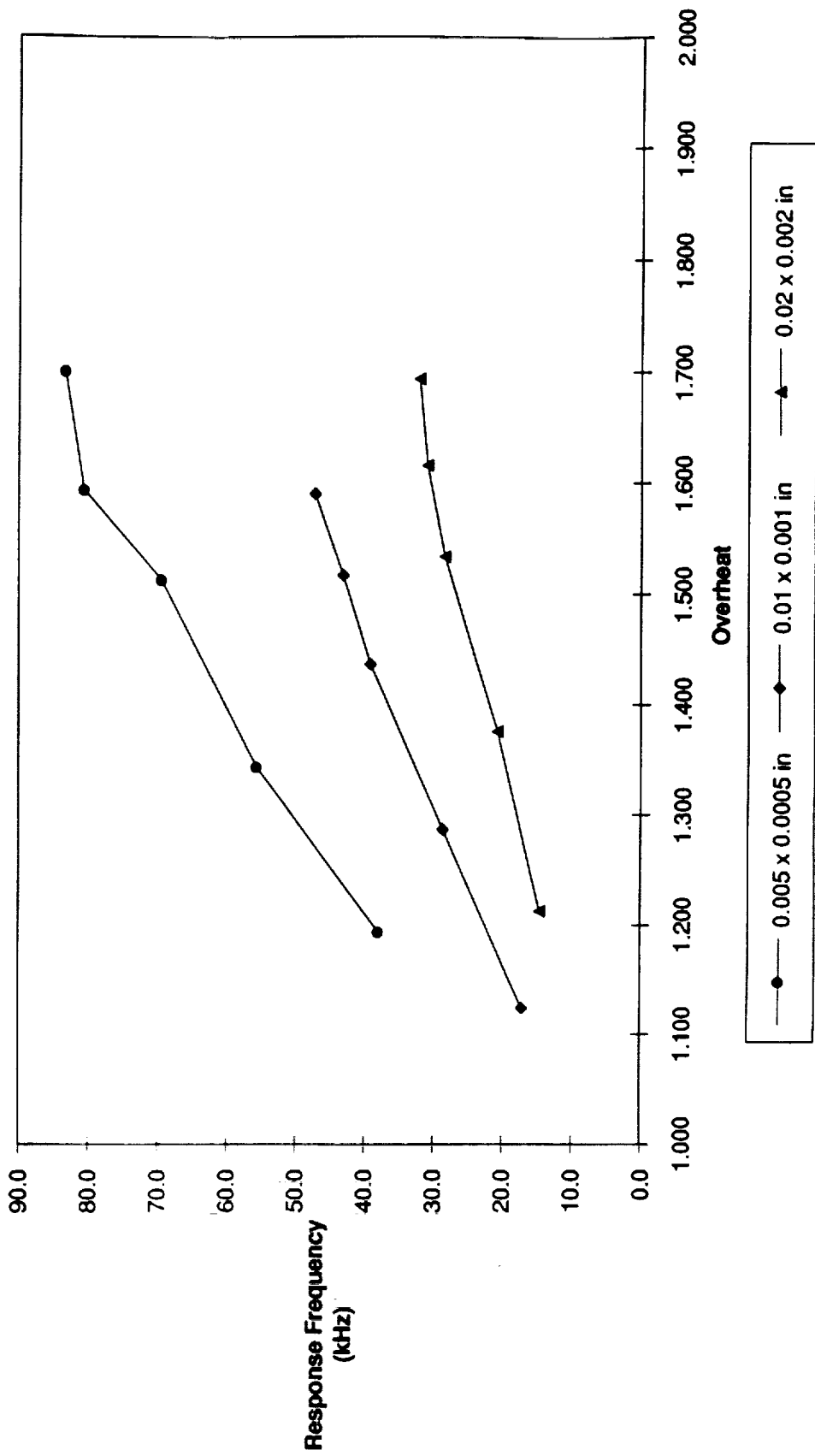
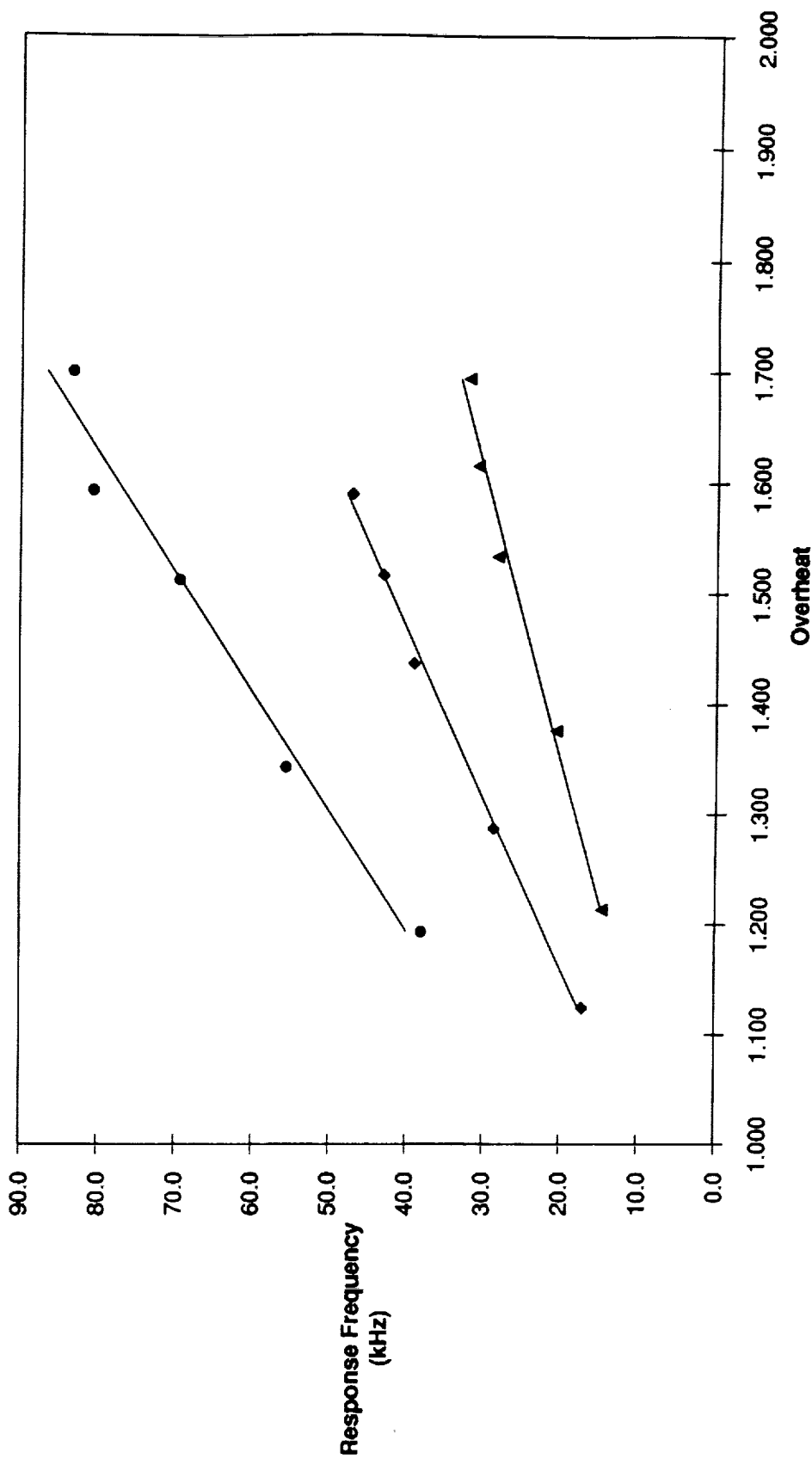


Fig 32

**Linearized Effects Of Increasing Overheat On Sensor Frequency Response
(Anemometer II)**



$\bar{F}_{16} \geq 3$

Velocity Step To 97 m/s With Overheat Of 1.68

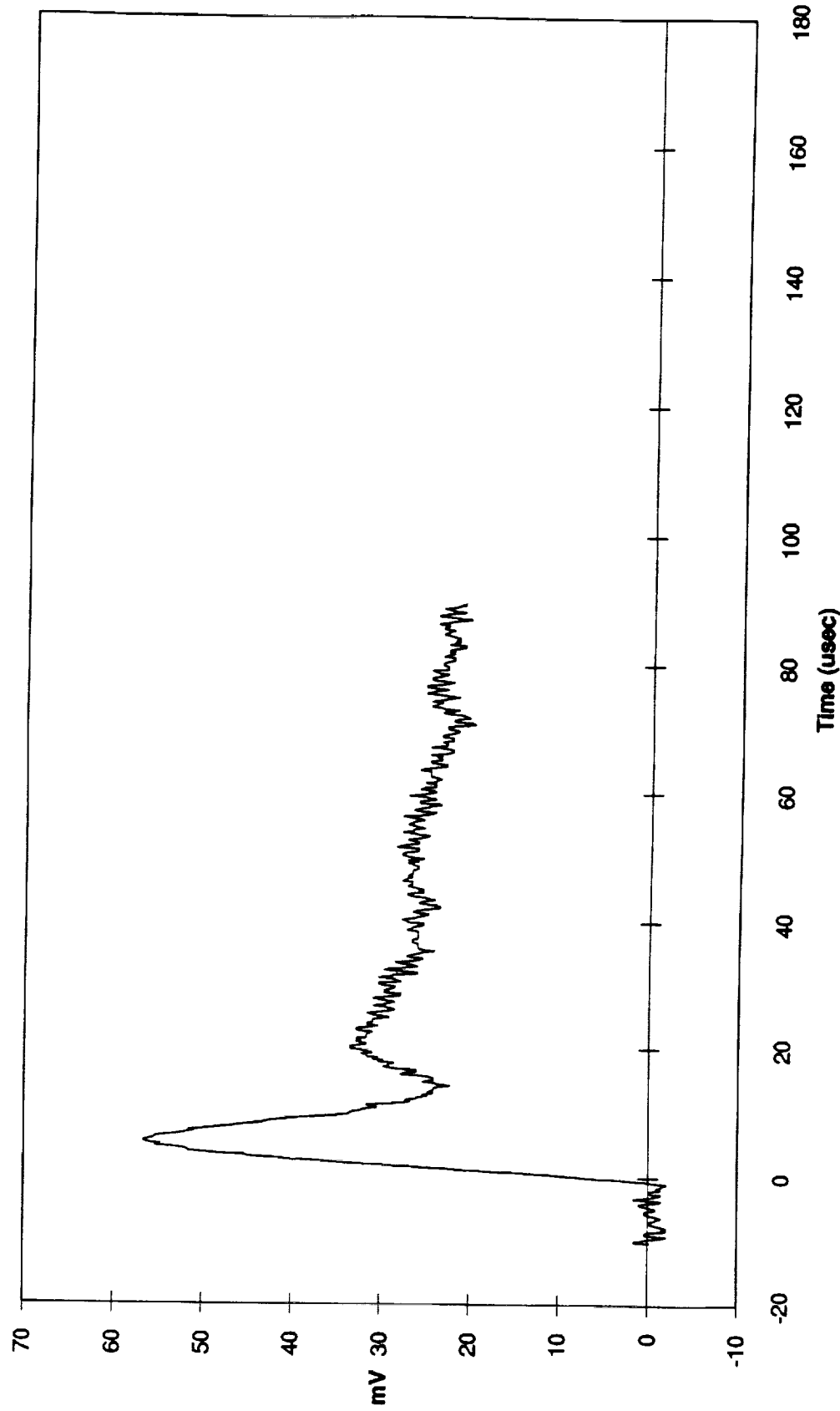
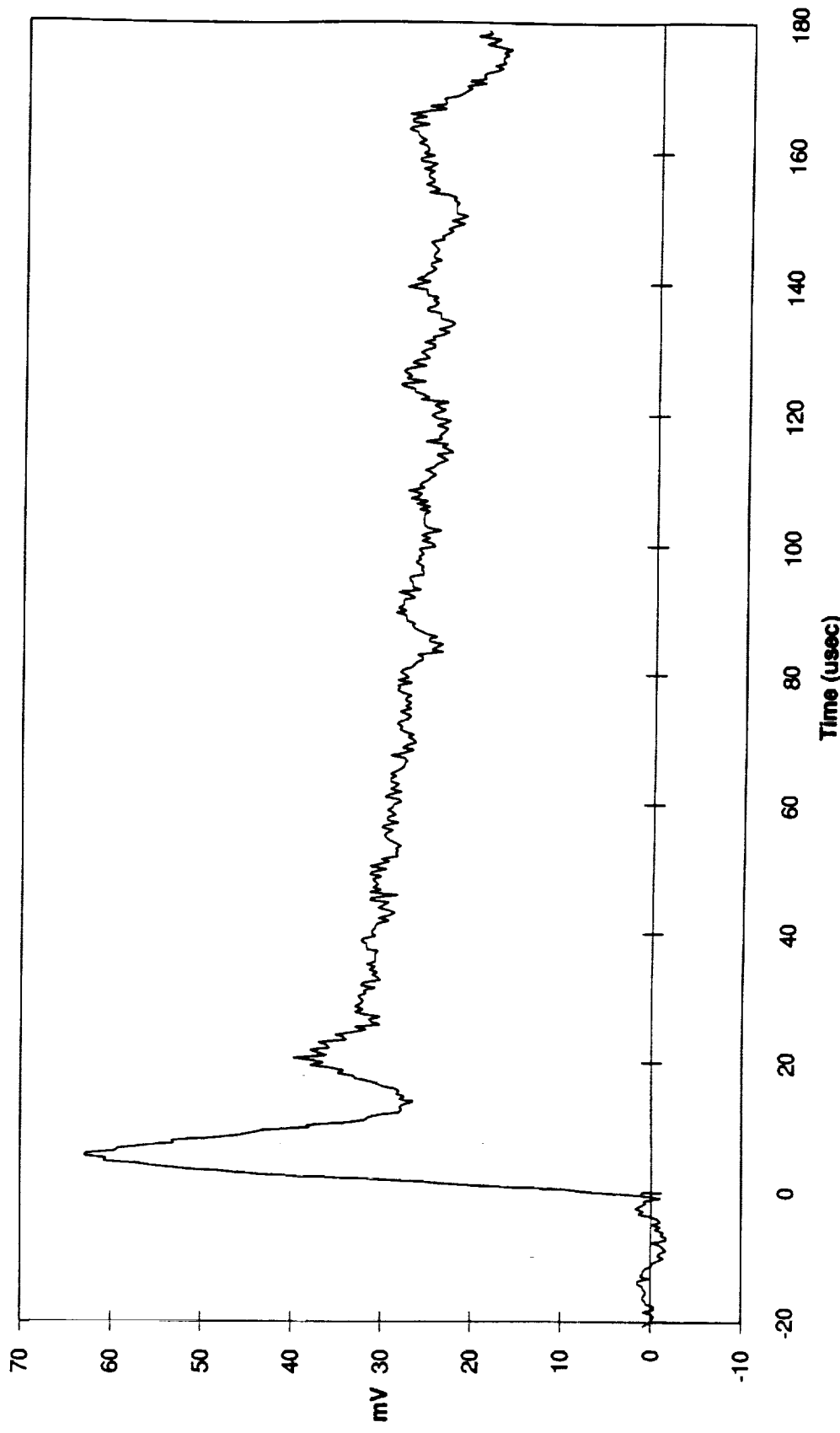


Fig 24

Velocity Step Of 113 m/s With Overheat Of 1.68



F-16 35

Velocity Step Of 114 m/s With Overheat Of 1.68

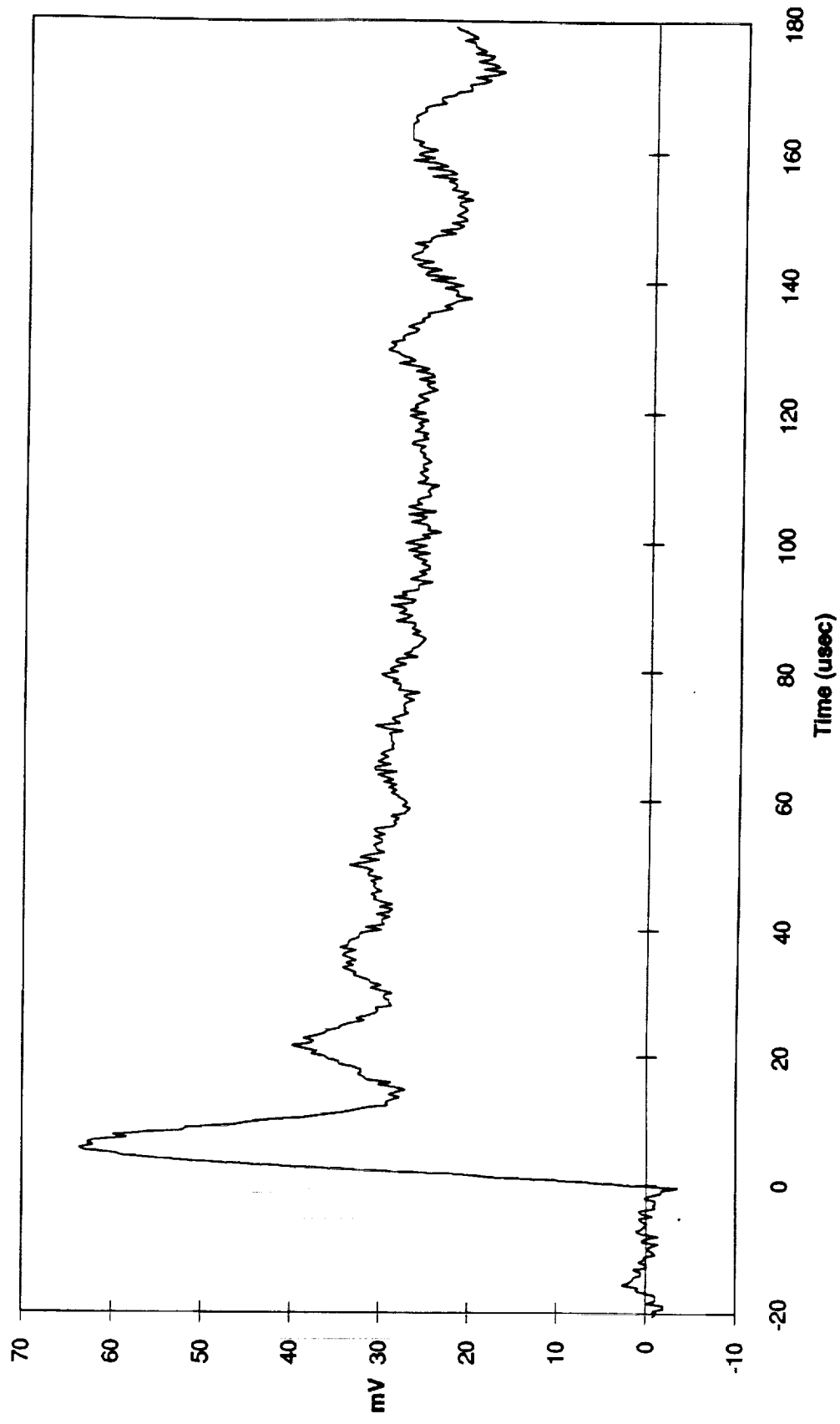


Fig 36

Velocity Step To 115 m/s With Overheat Of 1.68

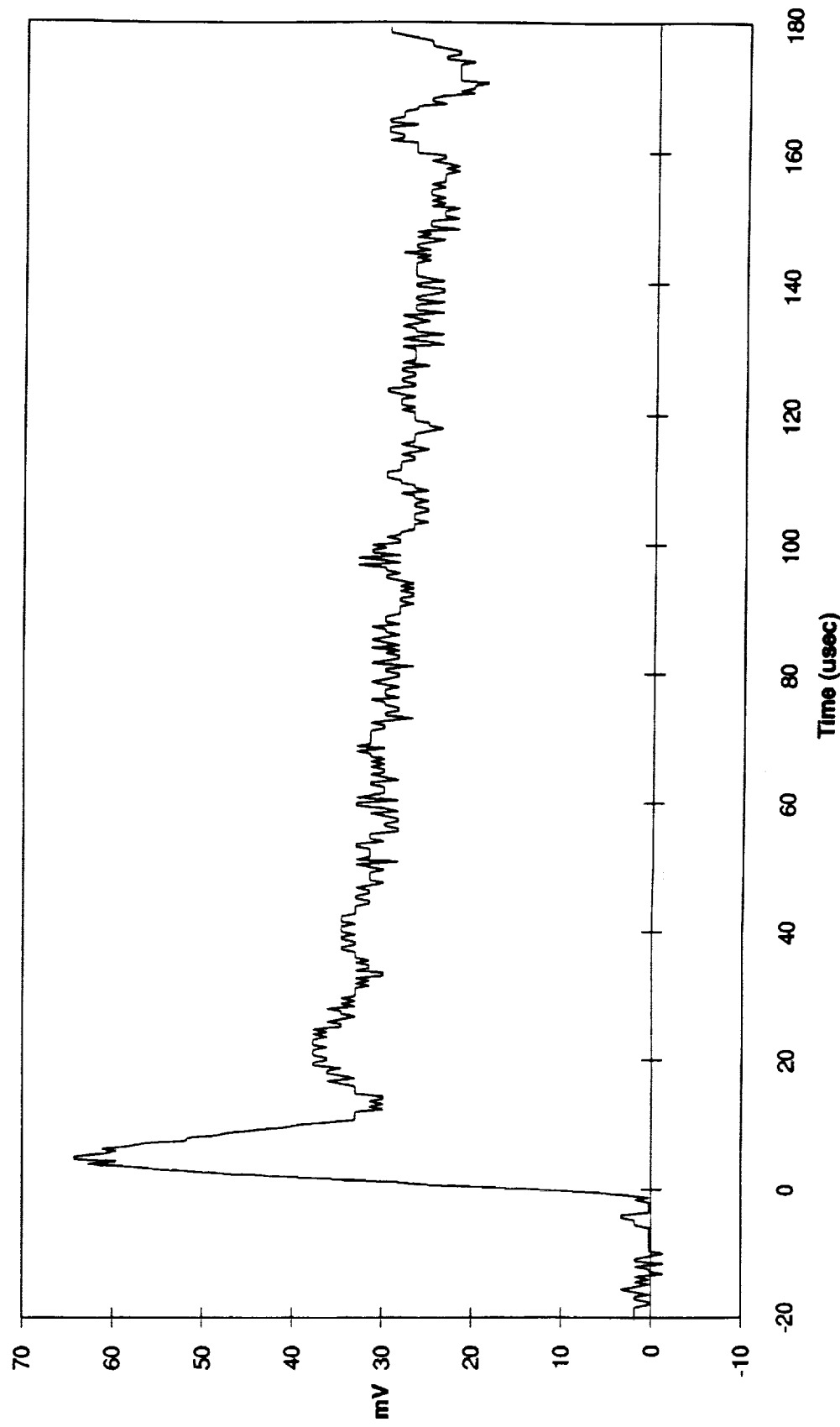


Fig. 37